Development of an Extended Logging Tool for Geothermal Exploration and Field Development

CALIFORNIA ENERGY COMMISSION

CONSULTANT REPORT

MARCH 2002
P500-02-073F

Gray Davis, *Governor*

CALIFORNIA ENERGY COMMISSION

Prepared By:

Electromagnetic Instruments Inc. (EMI)
1301 S. 46th St. UCRFS
Bldg. 300
Richmond, CA 94804

Contract No. 500-97-034

Michael Wilt, Ph.D.

Prepared For:

Elaine Sison-Lebrilla,
Resource Manager

Gail Wiggett, Ph.D
PIER Renewables Team Lead

Terry Surles,
PIER Program Manager

Steve Larson,
Executive Director

Legal Notice

This report was prepared as a result of work sponsored by the California Energy Commission (Commission, Energy Commission). It does not necessarily represent the views of the Commission, its employees, or the State of California. The Commission, the State of California, its employees, contractors, and subcontractors make no warranty, express or implied, and assume no legal liability for the information in this report; nor does any party represent that the use of this information will not infringe upon privately owned rights. This report has not been approved or disapproved by the Commission nor has the Commission passed upon the accuracy or adequacy of the information in this report.

Acknowledgement

We acknowledge assistance from geologist Mike Morea and reservoir engineer Dale Julander in the geologic interpretation of the Lost Hills data. We wish to thank Stuart Johnson and Caithness Energy for access to wells 66-21 and 68-23 in Dixie Valley, Nevada and for support in doing the field survey. Finally, we acknowledge the support of LLNL field engineers Pat Lewis and Duane Smith for aiding in tool deployment at Lost Hills and Dixie Valley.

Table of Contents

Figures

Preface

The Public Interest Energy Research (PIER) Program supports public interest energy research and development that will help improve the quality of life in California by bringing environmentally safe, affordable, and reliable energy services and products to the marketplace.

The PIER Program, managed by the California Energy Commission (Commission), annually awards up to $62 million to conduct the most promising public interest energy research by partnering with Research, Development, and Demonstration (RD&D) organizations, including individuals, businesses, utilities, and public or private research institutions.

PIER funding efforts are focused on the following six RD&D program areas:

- Buildings End-Use Energy Efficiency
- Industrial/Agricultural/Water End-Use Energy Efficiency
- Renewable Energy
- Environmentally-Preferred Advanced Generation
- Energy-Related Environmental Research
- Strategic Energy Research.

What follows is the final report for the Public Interest Energy Research (PIER) Project # 500-97-034 conducted by Electromagnetic Instruments Inc. (EMI). The report is entitled: “Development of an Extended Logging Tool for Geothermal Exploration and Field Development”. This project contributes to the Renewable Energy Research program.

For more information on the PIER Program, please visit the Commission's Web site at: http://www.energy.ca.gov/research/index.html or contact the Commission's Publications Unit at 916-654-5200.

Executive Summary

Inductive resistivity logging has long been an important technology to oil and gas producers because of the sensitivity of electrical resistivity to geological structure and variations in reservoir fluids. Electrical resistivity data from well logs is used in geologic description of reservoirs and in selecting producing intervals in wells. Unfortunately, commercial logging tools of this type are seldom used by geothermal developers because they are not made to withstand the hostile high temperature environment in geothermal boreholes. If such tools were available this would provide additional stimulus for development of California's abundant geothermal resources.

An additional important problem in geothermal field development is the mapping of producing fractures. This is a critical need because fractures play such an important role in accessing and producing geothermal reservoirs. Locating, orienting, and assessing producing fractures can guide drilling programs and optimize the placement of production and injection wells. This results in fewer dry holes and improved production in successful holes, substantially reducing cost and time in field development. Again, there are no commercial logging tools to fill this need. We note that the cost of a geothermal well ranges from one million dollars for a replacement well in a moderate depth known field to more than 10 million dollars for a deep exploration well. Given that exploration and drilling costs can account for up to forty per cent of the capital costs of producing geothermal-based electricity, it is evident that any tool or method that may reduce these up-front costs is likely to be of significant interest to the industry.

This report describes the design, construction, field-testing and commercialization of a new induction logging tool for geothermal exploration. The new device, termed GeoBILT (Geothermal Borehole Induction Logging Tool), is based on a California developed and Japanese owned prototype, called the MAIL system.

The new tool is more powerful, versatile, reliable and easier to use than its predecessor. In addition, the data gathered may be used for fracture mapping and single borehole imaging rather than simple resistivity logging. GeoBILT features a three-component borehole transmitter and a three-component variable-offset receiver whereas the older system featured only a one component transmitter and a single receiver offset. These unique features, presently unavailable with any commercial logging system, allow the collection of nine component "vector" data sets, which are crucial for the delineation of off-axis structure fractures and reservoir inhomogeneities. The multicomponent antennas also allow for effective logging in highly deviated or horizontal boreholes, which again is not possible with conventional tools or with the earlier prototype. The earlier system was designed for detecting fractures, whereas with the new system we can also image them. Finally, GeoBILT is engineered to operate at temperatures up to 260 °C and at depths up to 4 km.

The present array of exploration technology available to the geothermal field developer consists largely of surface-based geophysics and geological studies derived from outcrops

and well data. These tools provide a geological framework for the geothermal resource and often specific geophysical anomalies related to the rock alteration or the high temperature of the resource, but resource evaluation and well siting tools are lacking for geothermal.

Most well logging technology available to geothermal is a limited version of oil exploration tools. These "soft rock" logging tools are typically not designed to evaluate the structures of most interest in geothermal fields, i.e,. through-going fractures and faults, and often cannot operate in the high temperatures of geothermal boreholes. Conventional geophysical logging tools assume roughly flatlying structure, common to the oil fields. The tools are designed to provide formation evaluation of smoothly varying geology and locally horizontally layered (1D) sequences. In more complex geology, such as is associated with tectonically active geothermal fields, the tools provide incomplete and often misleading results..

With the limited array of tools available, the geothermal exploration manager must site and complete exploration wells that can cost up to 5 times an oil well drilled to the same depth This is because of the hard rock formation, hostile high-risk downhole conditions and the need for additional safety equipment. In addition, the possibility of missing productive zones in geothermal wells is much higher than in oil wells, because the production is often controlled by thin, steeply dipping fractures and igneous dikes rather than more flatlying horizons.

We believe that this new 3D induction logging technology can significantly reduce exploration costs by making the most of existing and new wells. Better logging technology can improve evaluation of the resource near the well and help site new wells. Because of the lack of appropriate logging technology for geothermal exploration, the overwhelming expenditure is in the drilling of exploration wells. This expense can easily be reduced by 20-30 percent by making the most of existing wells through logging.

Design, manufacture, testing and field demonstration of GeoBILT took two years. The vast majority of design and construction work was completed at EMI headquarters in Richmond, California. Design details are provided in Appendix A. Interpretation software and assistance in field-testing were undertaken by our national lab partners Lawrence Livermore National Laboratory and Sandia Laboratories.

Tool manufacture was completed in May 2001. In summer 2001 the tool was extensively calibrated and tested at a special logging instrument test facility in Houston, Texas. During the test, we measured tool performance under a variety of conditions and acquired calibration constants required to interpret field data. The final test was made in the test borehole where GeoBILT data was compared to numerical modeling results. GeoBILT's performance closely matched the expected results except at the highest frequencies.

We first tested the tool at the Lost Hills oil field in southern California, in the summer of 2001. We deployed GeoBILT in a fiberglass-cased observation well adjacent to a water injector used for pressure maintenance in the oil field. The injected water causes formation changes in the injection interval that results in a 3D resistivity structure near

the observation well used in the logging. The environment is a low temperature vertical well, providing very benign conditions for the first test.

Excellent quality field data were collected with GeoBILT for this test. Repeated logs showed a low noise and error level in the tool. The data were consistent with the known reservoir structure in zones unaffected by the flooding but GeoBILT provided excellent details on the direction of the injected water and its distribution near the well used in logging. We used a 3D modeling code to interpret the data, which indicated the direction and extent of the water flooding at the well.

With the 3D modeling we were able to determine the thickness of the flooded interval, the direction of primary flow in the interval and the changes in saturation. These important formation data are unavailable with traditional logging tools. This is a major departure from the routine analysis that comes with traditional logging data.

The 3D modeling is especially valuable in a geothermal setting because the geology is not a simple uniform structure and a traditional log can provide unsatisfactory results. For example, California's, geothermal environments range from the volcanic settings in Coso Hot Springs and Medicine Lake Highlands to complexly deformed metamorphic and volcanic rocks at The Geysers, to the soft rock, sedimentary environments in the Imperial Valley.

The second GeoBILT field test was a high temperature experiment at the Dixie Valley geothermal field in central Nevada. In this test, exploration well 66-21 was logged and the tool was exposed to temperatures up to 220 ^{o}C. The tool logged a 1000- ft interval several times in an area where near- well fractures were suspected to encounter the well. These fractures, which are likely associated with intrusive dikes, were clearly detected with the tool. In addition GeoBILT data provided an estimation of the strike and dip (geometric position) of these structures.

We feel that this technology can provide a powerful benefit to geothermal and to oil and gas development in California and potentially worldwide. The next step is to introduce the technology in a series of professional presentations followed by a series of field demonstrations. A commercialization plan for the utilization of the tool is attached with this report.

There is considerable industry interest in this technology for both geothermal and oil and gas applications. There are initiatives to apply GeoBILT at the Geysers for tracing reinjected fluids and at Coso Hot Springs for mapping induced fractures. In the oil fields we have had inquiries from the San Joaquin Valley for tracking water floods and from Canada for use in steam floods. We stress, however, that GeoBILT is fundamentally an R and D tool, designed to demonstrate the technology. It is therefore not a suitable instrument for heavy commercial use. For this purpose we need to build several copies of the tool. This is an ongoing project.

Abstract

The GeoBILT (Geothermal Borehole Induction Logging Tool) provides for fracture mapping and 3D formation evaluation from within a single well. The tool features a three-component borehole transmitter and a three-component variable offset receiver for collection of nine component “vector” data sets, which are crucial for the delineation of off-axis structure fractures and reservoir inhomogeneities. This also allows for effective logging in highly deviated or horizontal boreholes. GeoBILT is engineered to operate at temperatures up to 260 ° C and at depths up to 4 km.

GeoBILT was designed and manufactured at EMI headquarters in Richmond, California. Lawrence Livermore National Laboratory and Sandia laboratories, contributed in the development of interpretation software and assisted in field testing. The tool was completed in May 2001 and calibrated and tested in July.

The first field application took place in 2001 at the Lost Hills oil field in southern California. GeoBILT was deployed in a fiberglass-cased observation well adjacent to a water injector used for pressure maintenance. The injected water causes formation changes resulting in 3D resistivity structure near the observation well. The data were interpreted using a 3D modeling code. The results were consistent with the known reservoir structure and GeoBILT provided details on the flow direction of the injected water in flooded intervals. The second field application was made at the Dixie Valley geothermal field where the tool was deployed in high temperature wells. In this test we were able to detect throughgoing fractures associated with subsurface flow and hydrothermal alteration.

1 Introduction

1.1 Background and Overview

Inductive resistivity logging[1] has long been an important technology to oil and gas producers because of the sensitivity of electrical resistivity to geological structure and variations in reservoir fluids. Electrical resistivity data from well logs is commonly used in geologic description of reservoirs, in selecting producing intervals in wells and in estimating the type and quantity of fluids in the reservoirs. Unfortunately, geothermal developers do not often use commercial tools of this type, because they are not made to withstand the hostile high temperature environment in geothermal boreholes. This means that this essential tool for formation evaluation and reservoir delineation is unavailable to geothermal developers unless the boreholes are cooled before measurement.

A second important problem in geothermal field development is the mapping of producing fractures and other high permeability zones. This is critical because fractures play such an important role in accessing and producing geothermal reservoirs; successful wells often depend upon intersecting producing fractures. Locating, orienting, and assessing these structures can guide drilling programs and optimize the placement of production and injection wells. This results in fewer dry holes and better completion schedules in producing wells, which yield substantial cost and time savings in field development. Again, there are no commercial logging tools to fill this need.

In this report, we describe the design, construction, field testing and commercialization of a new induction logging tool for geothermal exploration in California. The new device, termed GeoBILT (Geothermal Borehole Induction Logging Tool), is based on an American (California) developed and Japanese owned prototype developed in the early 1990's (Sato et al, 1993; Wilt et al, 1997).

The new tool is more powerful, flexible, reliable and easier to use than its predecessor. In addition, the data may be used for fracture mapping and single borehole imaging rather than simple resistivity logging. GeoBILT features a three-component borehole transmitter and a three-component variable offset receiver. These unique features, presently unavailable with any commercial logging system, allow the collection of nine component "vector" data sets, which are crucial for the delineation of off-axis structure fractures and reservoir inhomogeneities. The multicomponent antennas also allow for effective logging in highly deviated or horizontal boreholes, which again is not possible with conventional tools. Finally, GeoBILT is engineered to operate in boreholes at temperatures up to 260° C and at depths up to 4 km.

[1] A brief review of induction logging principles is presented in Appendix B.

The multiplicity of data provides the opportunity to do sophisticated modeling from within a single borehole. In theory the tool should allow us to do three-dimensional imaging and fracture delineation from a single well. In practice there are several obstacles to this objective. The first is that no software is available to do this. Existing software inversion package are designed primarily for the crosswell configuration, and these need to be modified to work for a single well tool. The second is that 3D inversion requires significant computational capability. A 3D inversion is very computationally intensive and we anticipate that each inversion could require more than a week of computer time.

These software objectives are as challenging as the hardware goals but they must be addressed in parallel to have codes ready for field demonstrations. We have therefore enlisted Lawrence Livermore National lab and Sandia National labs as partners to help us develop a software package capable of 3D imaging and fracture delineation.

The final software package includes both a simple processing algorithm for 1D analysis and model simulation, and a more sophisticated package for detailed reservoir modeling and data inversion.

1.2 Project Objectives

The overall objective of this project is to develop an induction (resistivity) logging tool for geothermal application that will detect 3D formation structure and delineate near well fractures. The three-year project is organized into five stages:

- Tool Design - this involves the design of all hardware and software components of the operating tool. The final product is a set of plans.

- Tool Manufacture - this involves the manufacture of the tool. The final deliverable is the completed tool.

- Calibration and Testing - at this stage, parts of the tool are tested and lab and field calibration are performed. The final deliverable is an operations manual.

- Field Demonstration - phase 1 of the demonstration is conducted at a carefully chosen low temperature site where the system can be exercised and the results compared to other data. Phase 2 test is at a more hostile high temperature geothermal site. The final deliverables for these phases are the compiled and interpreted field results.

- Commercialization - a plan for commercializing the technology is presented.

In parallel with the hardware development and field application, we are providing a set of software tools for data interpretation.

- 1D Code - this code will provide a layered model tool response
- 3D Code (Forward)
- 3D Code (Inverse) - there are two types: Full Inversion and Fast Inversion. For the Full Inversion, we plan to adapt existing 3D inverse codes to the single well case. We also plan to develop a faster version since the Full Inversion is very computationally intensive. This Fast Inversion could be capable of providing results in the field.

1.3 Report Organization

In this report, we describe the design, manufacture and field test results of the GeoBILT prototype. In general, this report will describe the tool development from the design stages to field deployments, emphasizing on the main system features, accomplishments and field results. Design and manufacturing details are provided in the attached appendices.

The report is organized into three main sections and three appendices. In the main body of the report, we cover general tool design and manufacture, field deployments and data interpretation. In the appendices we describe the tool design in detail and provide a short tutorial on induction logging.

2 Project Approach

The deliverables for this project are: (1) a completed and tested logging device, (2) the design documents, manuals, and (3) this report. To achieve these goals, careful planning was needed. We also collaborated with outside researchers and contractors at the earliest stages of the research.

This chapter describes the highlights of the major features and the capabilities that distinguish GeoBILT from other more traditional logging tools. The development plan we followed to accomplish the final design is also described here.

2.1 Overview of Hardware Design

2.1.1 Background

The initial concept of induction logging in a geothermal environment came from Japanese-US collaboration in the early 1990's. A series of projects between EMI and Japanese company GERD (Geothermal Energy Research and Development) resulted in a series of prototype logging devices that were tested in Japan and the US. (Sato et al, 1996; Wilt et al., 1997). The first tool developed was the MFT (Multi-Frequency Triaxial). This device had an axial transmitter and a single three-component receiver offset 6m from the source. The second tool was the MAIL (Multiple Array Induction Logger). This tool featured several axial receivers and a single transaxial receiver from a single axial transmitter. Both tools were designed for geothermal applications and successfully tested in high temperature boreholes.

The tests from these tools provided intriguing results but it was also discovered that both of these devices had serious flaws and limitations (Wilt et al., 1997). These tools could potentially detect fractures and near well 3D structure but were unable to delineate the structure because of insufficient data coverage and inadequate data quality. In addition, the tools did not work very effectively at high frequencies due to ineffectual isolation and shielding.

We used experience gained from the development of these tools in the design and manufacture of GeoBILT. In fact, the GeoBILT design was initially based on the Japanese prototype, the MAIL .We found, however, that this design was not sufficient and we had to use other resources such as numerical modeling and sensitivity studies to obtain an appropriate tool for 3D imaging. For example, sensitivity analysis made by Alumbaugh and Wilt (2000) showed the importance of multiple sensor spacings and multi-component source and receivers in developing a 3D model.

Because of this process, the design of the new tool differs from the MAIL in several significant ways. GeoBILT has a three-component transmitter and an array of three-component receivers, spaced logarithmically. We also used experience gained from earlier field trials to properly isolate the transmitter from the receiver signals and to properly shield sensors and wiring. In particular, we found the following list to be most crucial.

- Transmitter and receiver sections need to be carefully electronically isolated to insure high data quality;
- Multiple source-receiver spacings are required for imaging;
- A three-component transmitter is required for fracture delineation and 3D imaging;
- Multi-component source and receivers need to be wound coincidentally; that is, the three-component coils must be wound around a common center position.

2.1.2 Design of GeoBILT

GeoBILT is designed so that the signal generation and data processing are mainly accomplished downhole. The surface station provides power, gives digital commands and receives a digital data stream from the tool. The simple surface facilities mean that the tool can operate from a variety of logging platforms and can therefore be transported worldwide without loss of usability.

The tool consists of five separate sections: three electronic compartments and two antenna units (Figure 1). All of the electronic sections are housed in vacuum insulated dewars. These dewars are basically thermos bottles that isolate the interior from the exterior. In a high temperature environment, the interior temperature increases at roughly six ^{o}C / per hour. This provides an operating range of 12-14 hours before cooling is required. Note that the circuits are cooled simply by opening the dewar and exposing them to the outside air.

The housings for the antennas are made of a special high temperature fiberglass composite material that is stable up to 260 ^{o}C. High temperature solder is also used for all electrical connections. The O-rings and greases used are stable at high temperature and minimize heat transfer.

The source antennas are coincident, multiturn coils wound around a common center with matched inductances, allowing them to be tuned with a single set of capacitors. The antennas are air-core coils wound around a machined frame made

of high temperature fiberglass. They are roughly 1m long and the magnetic moment[2] of all of the sources is approximately 10 A-m^2. This is sufficient source strength for operation at source-receiver offsets of up to 50m.

The transmitter signal is generated downhole using a driver circuit controlled by the clock. The driver is basically a very efficient power supply switch that generates a square wave signal with a minimum of heat dissipation. The tool operates at 4 four frequencies (2, 6, 16 and 42 kHz). At each frequency, the downhole computer selects a capacitor to connect in series with the coil. This capacitor tunes the coil, thereby dramatically reducing the impedance at the tuning frequency, and thereby increasing the current. Capacitive tuning of the square wave signal also results in the sinusoidal transmitter waveform.

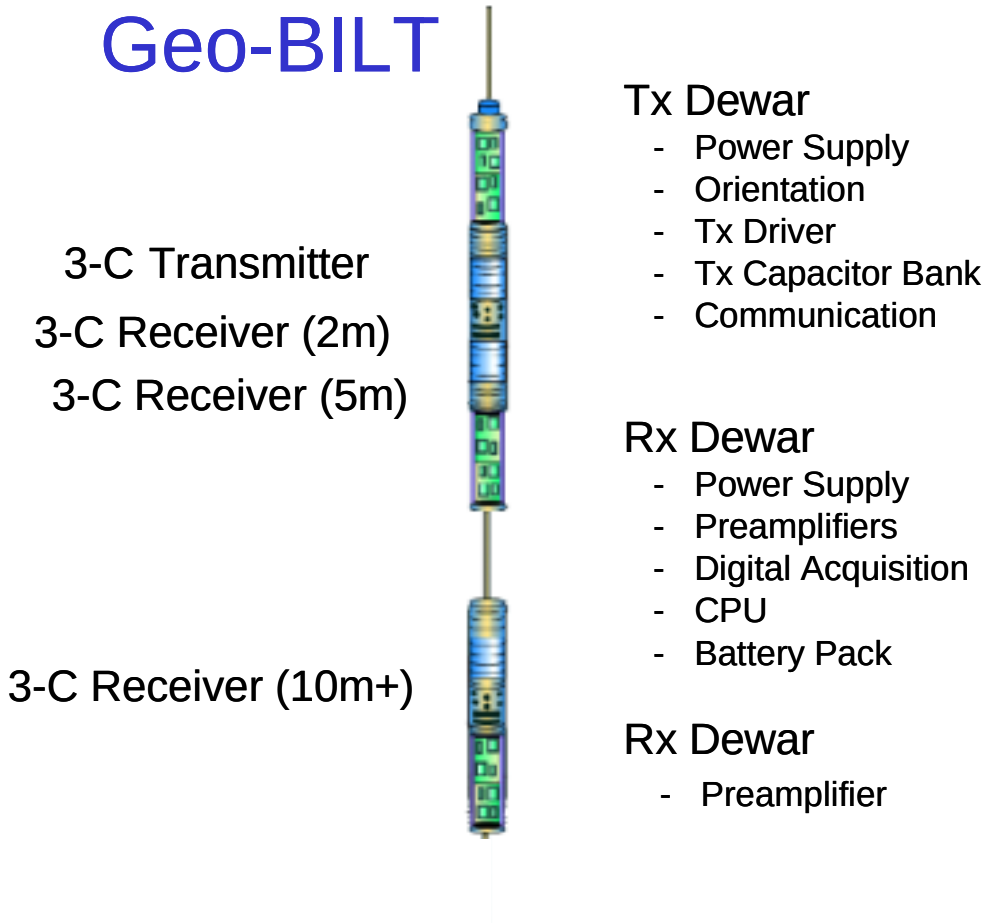

Figure 1. Schematic Diagram of GeoBILT

[2] The magnetic moment of an induction coil is a measure of source strength (or sensitivity). It is defined as the product of the effective cross-sectional area, the number of windings and the current in the windings.

GeoBILT has three three-component magnetic induction sensors separated at 2, 5, and 10m+ from the source. The lower sensor package is suspended on the logging cable. These sensors are multiturn coils each wound around a common center. The axial receivers are simple multiturn coils wound around a base; the transaxial receivers are made of small coils 3 inches by 1.5 inches with a mu-metal core (see Appendix A). The sensors and attached amplifiers are designed for optimum sensitivity in the frequency range of 2-50 kHz.

GeoBILT also features a three-component magnetometer and accelerometer package for tool orientation. Three separate toroidal sensors are used as transmitter current monitors, and a series of temperature and voltage sensors are used for assessing the operating conditions. The magnetometers are necessary for triaxial operation because the tool spins freely during logging. Before the data can be interpreted, it is required that the sensors be rotated to known positions. This is done mathematically through the magnetic sensors.

The signals are channeled from all receivers and sensors into a downhole analog to digital converter (A/D) and computer module. Data are first digitized by a 16-bit, 4-channel A/D and averaged on the downhole computer. The Fourier coefficients are then transmitted to the surface along with a selected stacked digital time series and the tool status data. These data are collected on a laptop computer connected to the surface station.

The surface station supplies power to the transmitter and receives digital signals from the downhole computer. Power for the receiver section is supplied by a downhole battery pack. The battery pack was added after initial system tests demonstrated that a higher isolation is needed between the source and receiver sections to eliminate stray coupling. This isolation was accomplished by reducing as many wire connections as possible between the source and receiver sections. The only remaining connection between the source and receiver sections is a transformer-isolated clock line and one shielded twisted pair for communication.

2.2 Overview of Interpretation Software

Field data interpretation consists of two stages. In the field, the operator requires immediate information to determine if the tool is working properly and what sections of the borehole are suitable for detailed analysis. For this purpose, a simple apparent resistivity algorithm provides real time results on the laptop PC used in logging. Once logging is complete, however, more detailed analysis of particular depth segments of the log may be warranted. For this purpose, more

sophisticated layered model analysis and 3D imaging and fracture mapping software are applied at a later time.

The first algorithm will calculate the apparent resistivity of the formation. These data, which are the primary output of a commercial induction log, are usually calculated from a simple analytical formula. However, due to the longer source-receiver offsets in GeoBILT (as compared to commercial logging systems) the standard algorithms are no longer appropriate. The apparent resistivity for this extended logging system requires a full mathematical solution to the problem of magnetic dipoles in a whole space, not just the low frequency approximation used in commercial algorithms. The full solution, while still in analytical form, is considerably more complex than the approximate solution and cannot be used to directly solve for the apparent resistivity (Hohmann, 1988). Our approach is to develop a simple inversion for the analytical expression that calculates an apparent resistivity to minimize misfit between the observed and calculated fields. This least squares solution may be easily implemented on the portable field computer and will operate in real time.

The second algorithm to be developed is a code to resolve formation bedding. This code involves a least squares inversion for a layered model structure. It is a fairly straightforward algorithm utilizing a least squares inversion based on the one dimensional forward code EM1D (Lee, 1989). It will provide good bed boundary information for flat lying sections and, for other sections, it provides useful input to the 3D imaging code. In addition, when utilizing the three dimensional source and receiver antennas, the algorithm will provide some determination of formation anisotropy. This latter quantity is useful for determining microfracture orientation in hard rock environments and for estimating fluid saturations in soft rock petroleum reservoirs.

The final codes are more sophisticated analysis packages for single borehole imaging and fracture imaging. The three-component sources and multi-offset three dimensional sensors of the GeoBILT system allow for moderate to high definition of near well 3D structure. To accomplish this, we will adapt existing 3D EM modeling codes (presently in use at Lawrence Livermore National laboratory and Sandia laboratories) to the borehole environment. The code will also serve as the kernel for data imaging software. The output of this software is a three dimensional image of the resistivity distribution in the vicinity of the borehole.

Fracture imaging inversion is based upon a 3D model of planar structures that approximate fractures. The output of the fracture imaging code are the properties and orientations of throughgoing fractures and more general information on fractures that pass near the wellbore but do not cross it.

2.3 Development Plan

We accomplished the tool design, manufacture, testing and field demonstration for GeoBILT in a span of two years. This initial period was followed by a six-month demonstration and commercialization phase. The vast majority of design and construction work were completed at EMI headquarters in Richmond, California. Tool calibration occurred locally and at a commercial testing facility in Texas. Initial field testing occurred at the Lost Hills oil field in central California. A high temperature field demonstration was made in Dixie Valley, Nevada.

The development plan consists of five principal tasks: **1)** hardware and software design; **2)** system manufacture; **3)** development of imaging technology; **4)** testing of the device in field trials; and **5**) commercialization. In each task, there are a number of subtasks, each with specific objectives and milestones.

The project closely followed the design and manufacture timeline provided in the proposal. Delays were encountered during the testing phase when we found that the tool performance was below specifications due to strong direct coupling (ground loops) between the transmitter and receiver.

This coupling problem was solved by almost completely isolating the receiver section from the transmitter. The isolation was achieved by replacing the receiver power supply with internal batteries and using transformers to isolate the communication and timing link between the transmitter and receivers.

The engineering solution to the coupling problem delayed the calibration and field test for about three months. We feel that this effort was well worth the delay.

3 Project Outcome

In general, the GeoBILT project was a remarkable success. The tool was designed, manufactured and tested within the time and expense budget and it performed very well in field trials. In addition to the individual project success, this project has spawned renewed interest in the field of multi-component and extended logging (see bibliography).

In 1999, the project started with tool design and numerical modeling. Tool manufacture proceeded in 2000 and was completed in February 2001. Appendix A describes the design of the tool in detail.

In this section, we describe the deployment of the tool, the calibration results and the results of two field demonstrations. The first field test was conducted in a controlled oil field setting, and the second in a geothermal environment.

3.1 Tool Operation and Deployment

The GeoBILT borehole tool consists of three major sections that range from 12 to more than 23 feet long (Figure 1). Tool assembly is accomplished by laying the pieces horizontally on tool stands and fitting together the joints using hand tools; the process takes about an hour on site. When fully assembled, the tool is more than 45 ft long and must be hoisted as one piece. We have devised a special "rolling sling" for accomplishing this (Figure 2).

Figure 2. Field deployment of GeoBILT

The “rolling sling” was devised at EMI to hoist this long tool without overstressing the long antenna components or the tool joints. With the sling, the tool is anchored at two points: one near the tool head, and the second on the antenna section about halfway down the tool (Figure 2). After clamps are attached at these two points, the sling is tied between them and the crane hoists the tool using a pulley attached to the sling. This arrangement automatically distributes and adjusts the load during hoisting. When the tool is horizontal, the load is equally balanced between the two points and it progressively moves to the upper point as the tool becomes more vertical. Although quite simple in design, this device has permitted a number of successful safe tool deployments with no observed stress damage.

The tool is deployed using standard a 7-conductor wireline cable and an encoder/counter for depth control. Due to its length, a 60-ft crane is required for deployment. After assembly and initial testing, the tool is typically hoisted and positioned over the well. We then collect “free space" data at the frequencies selected for logging, and these data are used as part of the calibration corrections.

Two main logging modes are available for data collection. In the fast mode, only the vertical (axial) transmitter is activated, and data are collected on all sensors. For the complete mode, all three transmitters are activated, and data are collected on all sensors. The fast mode allows a quick survey of the well; the complete mode is for collection of detailed data to be used in 3D inversions.

The borehole is logged while the tool is moving. The logging speed ranges from 10 to 20 ft per minute depending on the frequency and the selection of fast or complete logging modes. At a rate of 10 ft/minute, we can obtain a full tensor measurement about every foot.

Prior to deployment the survey parameters are established from field simulations, usually based upon a geologic model provided by the client. From these considerations we select the depth interval for logging, the frequencies of operation and the logging speed.

3.2 Calibration of GeoBILT

The next step in the development of GeoBILT was to perform a complete calibration of the system. This procedure is crucial to the success of the tool in its application to 3D modeling.

With such an involved and large system, calibration was a difficult and complex procedure. In particular, we needed to measure the individual response of all sensors and sources as a function of temperature and frequency. We also needed to

measure the response of the system as a whole as a function of temperature and frequency.

Fortunately, we have access to an excellent testing facility available in Houston, Texas. This facility has the capability to calibrate and test the individual electronic and sensor components and to measure the response of the system as a whole. They also have a very well characterized well (customer acceptance test or "CAT" well) to run test logs in. The formation response in the well is very well known because it has been used in logging tests for more than 20 years.

The CAT well is in a well characterized flatlying formation characteristic of south Texas geology. The layered sequence consists of both thin and thick beds and has a resistivity variation from 5 ohm-m to more than 100 ohm-m. This provides an excellent testing environment for GeoBILT because it allows us to examine different aspects of the tool. For example, we can expect a difference between the horizontal and vertical logs in the thin beds but these logs should have a similar response in the thicker beds. We also expect a small response in the null components because there is very little 3D structure and the beds are flatlying.

One of the first system tests of GeoBILT is the lift experiment. Here, the tool is oriented horizontally with one of the transaxial sensors pointed upwards. Measurements are then made at two different heights above the ground where the conductivity of the ground is known. The difference between these measurements allows us to determine the free-air response and the effect of the conducting ground.

Some of the results of the lift test are provided in Figure 3 where GeoBILT response is compared against the calculated response for the formation at the Houston test site. The response is close to that predicted from the model at all frequencies except for the highest one. This was in general an encouraging sign.

GeoBILT was then run in the CAT well in a series of logs to establish system repeatability, noise level and frequency response. Again, these logs can be matched to predicted response from the formation distribution in the wells.

In Figure 4, the GeoBILT logs are plotted together with the reproduced logs from the CAT well. Here we show the comparison with the 2m and 5m axial logs at a frequency of 6 kHz (vertical component) to the predicted response, based on earlier logs. The match between these logs is remarkably close for both 2m and 5m logs, indicating that: 1) the GeoBILT response is well characterized and stable; and 2) the predicted formation response is accurate.

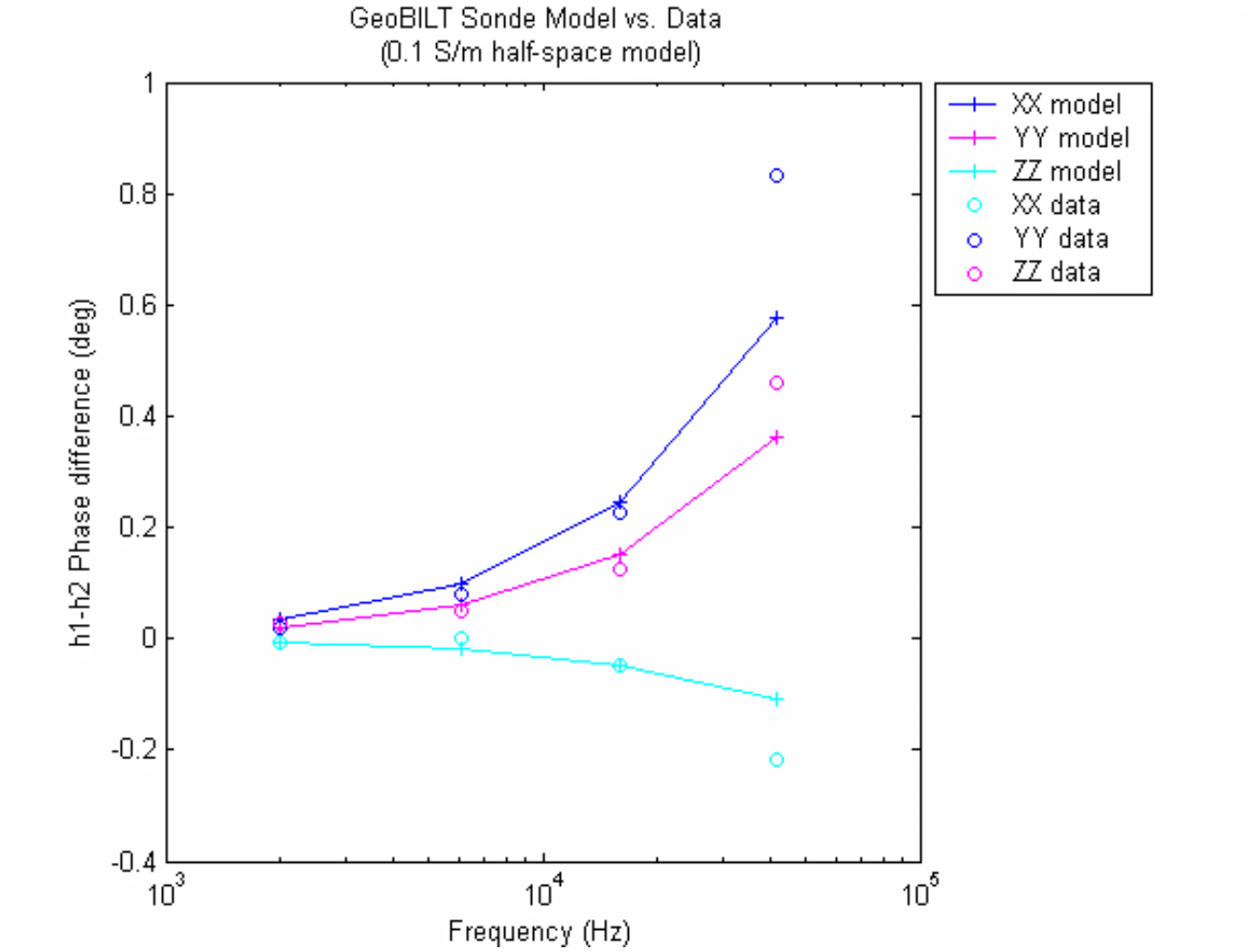

Figure 3. Comparison of GeoBILT response vs. free-air response at the test facility

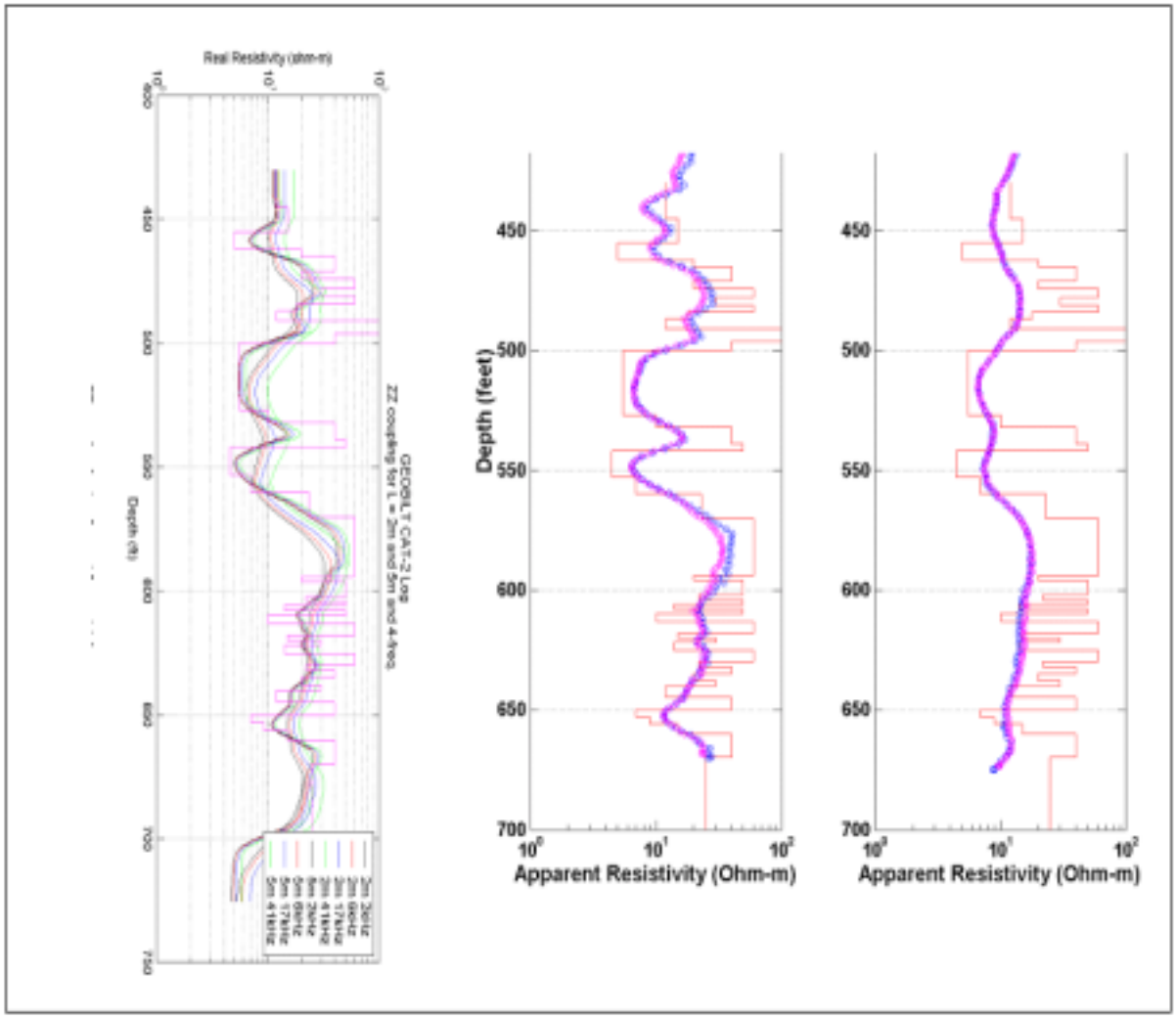

Figure 4. GeoBILT response (right) for maximum coupled axial receivers 2 and 5m are compared to numerical model results (left).

In Figure 5, the 5m horizontal component (transaxial) logs are compared against the predicted response. Whereas we can compare GeoBILT to a similar tool from the axial response, there is no equivalent tool for the transaxial data. The predicted formation response is based on a model derived from a closely spaced axial tool. It is therefore not as accurate as the axial response model

The GeoBILT response closely matches the theoretical response in controlled tests. The difference between these curves in several of the intervals suggests uncertainty in the formation model or some errors in the tool orientation system.

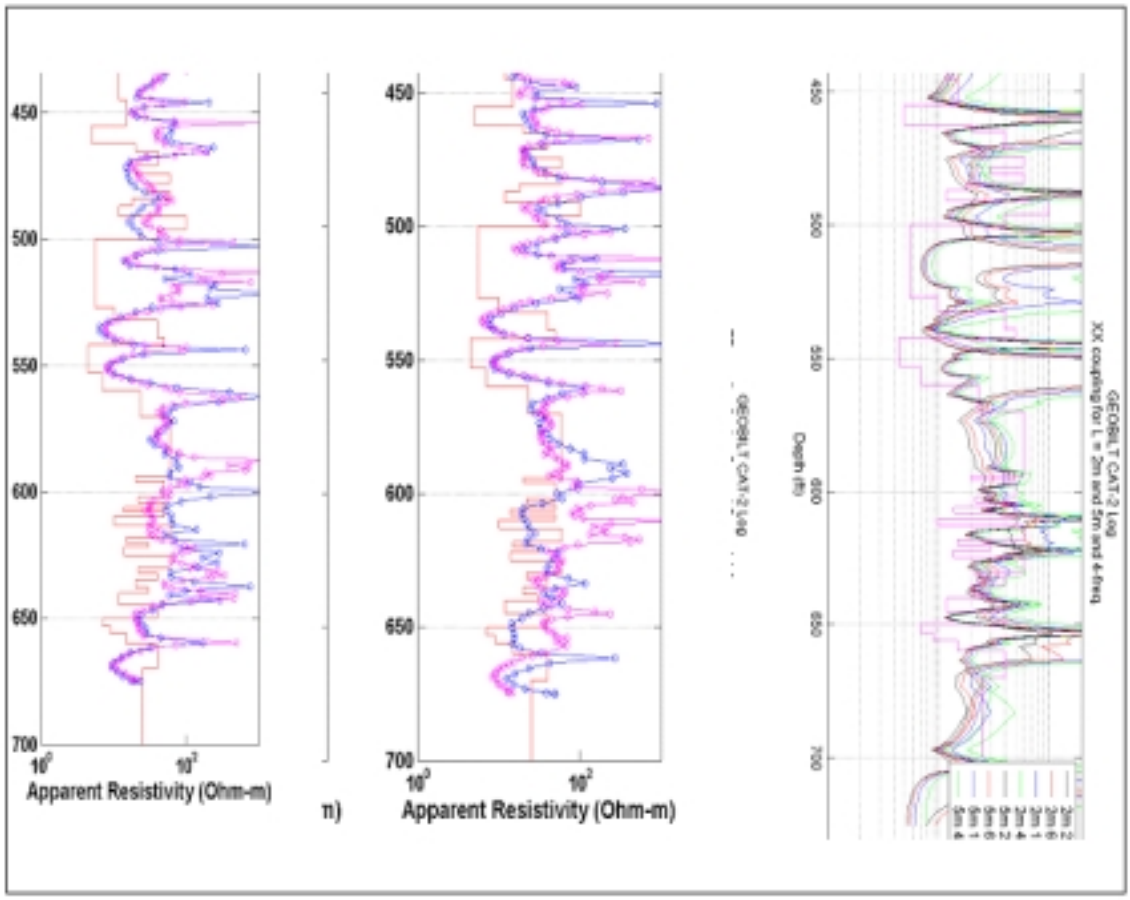

Figure 5. GeoBILT response (left) for maximum coupled transaxial axial receivers 5m compared to numerical model results (right).

The two-week calibration provided extensive data on the capability of the tool and its performance against known standards. The following were some of the significant findings:

- At the lower frequencies (2 and 6 kHz), GeoBILT performs at or above specification. The sensors have excellent sensitivity and the data repeats within a few tenths of a percent.

- The electronic systems show almost no drift with temperature; the sensors, however, show substantial drift and data needs to be corrected in a high temperature environment.

- At the high frequencies, particularly 42 kHz, the tool performance was disappointing. There is evidence of spurious coupling and drift in the transaxial components. It is unclear how much this affects future data interpretation.

- The magnetometers used for tool rotation performed adequately but they could be improved by applying the new temperature calibration constants.

In general, we found the calibration results satisfactory upon completion of the tests. GeoBILT was then ready for field demonstration.

4 Field Demonstrations

4.1 Case 1: Initial Field Trial at Lost Hills, California

The initial deployment of GeoBILT occurred on May 8-11, 2001 at the Lost Hills oil field in southern California at the leases operated by Chevron USA (Figure 6). Data were collected in a fiberglass-cased observation well adjacent to a water injector used for pressure maintenance. This site was selected based on the availability of the fiberglass wells and the favorable downhole environment, which includes the effect of the ongoing waterflood. The flood alters the resistivity structure due to the lower resistivity of the injectate, thereby creating 2D and 3D resistivity structures. These structures are excellent targets for interwell and single well imaging.

Both crosswell and single well EM data were collected at the site. The site features closely spaced vertical observation wells straddling and both within 100ft of the existing water injector. The existing waterflood has been effective in stabilizing the formation and in re-supplying the water phase.

Figure 6. Location map of field surveys in the San Joaquin valley

The field is about 4 hours drive from EMI headquarters in Richmond, California. This close proximity coupled with our excellent working relationship with Chevron USA personnel makes this is an excellent site for testing prototype instrumentation.

The Lost Hills oil field is located at the western margin of the San Joaquin basin in Kern County, California. Production is concentrated in the Pliocene Etchegoin Formation. and Miocene Belridge Diatomite of the Monterey Formation., which combined, account for original oil in place in excess of 2 billion barrels within a 1000 ft thick reservoir. The principal reservoir rock is a diatomaceous shale characterized by very low matrix permeability (0.1 to 1 m mdarcies) and a slightly higher permeability siltstone (Stosur and David, 1976). Both rocks are characterized by high porosity and oil saturation.

Most recovery operations at Lost Hills use induced fractures for better reservoir contact, and water flooding for pressure maintenance. Both production and injection wells are fractured in up to 5 depth intervals within the production zone. Oil recovery operations at Lost Hills have historically been characterized by low flow rates and inefficient sweep.

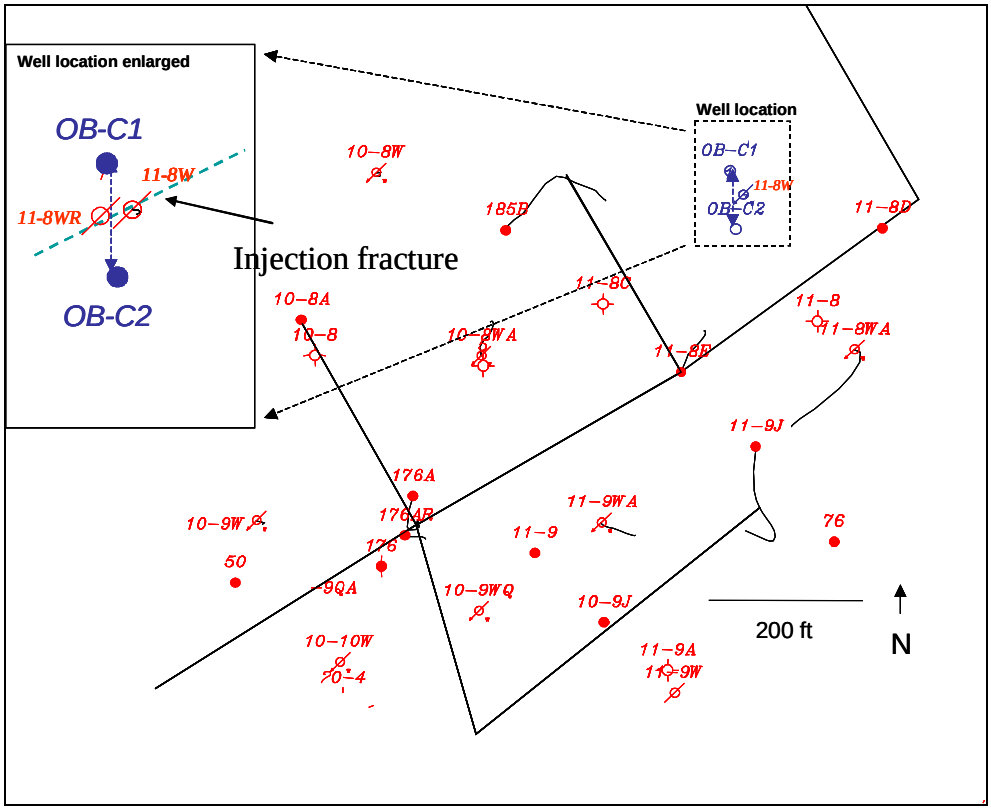

Figure 7. Well map, part of Lost Hills fields

The observation wells were drilled that straddle an existing water injector (11-8W) and an adjacent newly drilled well for CO_2 injection (11-8WR) (see Figure 7). Well 11-8W has been injecting water at the rate of 200-300 barrels/day throughout the production interval (1200-2000 ft) since 1994.

The injected water is a combination of produced water and make-up water from a shallower and less saline Tulare Formation. source. The overall fluid is 30 percent more resistive than the formation water but the injected fluid will still dramatically reduce the formation resistivity as it fills up void space or mobilizes oil or gas. In Figure 8, we show deep induction resistivity logs from wells 11-8w and 11-8wr. The difference between these two logs is the effect of the water injection near the wells. The logs indicate resistivity decreases of up to 50 percent in several layers where the water injection is significant. In particular, the F, H and K intervals show the greatest change due to the flooding.

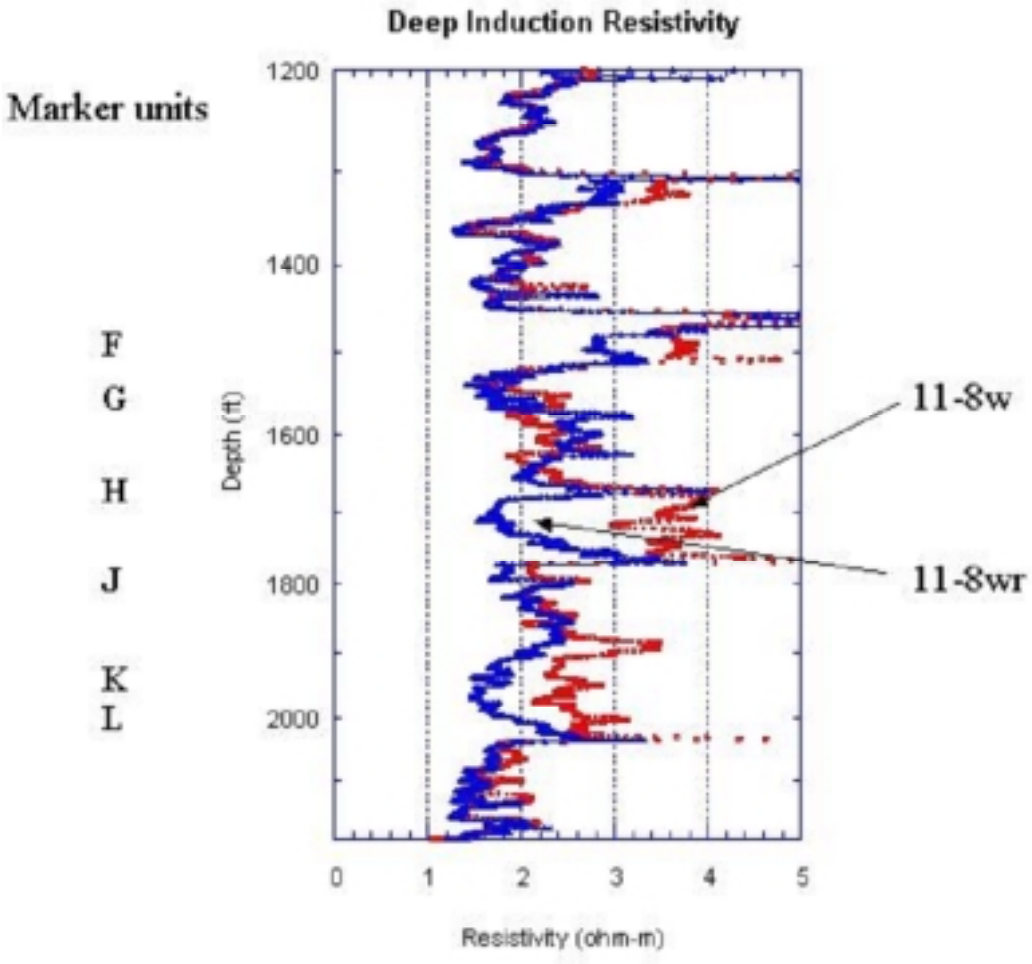

Figure 8. Comparison of induction resistivity logs between 11-8w and 11-8

4.1.1 Crosswell Data Collection

Crosswell data were collected with the XBH2000 system in August 2000 using well OB-C1 for the transmitter tool and OB-C2 for the receiver. Data were collected within the depth range from 1250-2100 ft, or the entire depth range completed with fiberglass well.

Data were collected in individual profiles where the receiver remains fixed and the transmitter moves between the depth ranges, broadcasting continuously while moving. After the profile is complete, the receivers are re-positioned and the process is repeated until all source and receiver positions are occupied. The receivers are spaced every 17 ft and the transmitters spaced every 4 ft within the depths of interest. Data were collected using a frequency of 760 Hz; we stacked the signal 500 cycles for each measurement.

Each profile required roughly 55 minutes to collect and re-position the sensors. The entire data set was collected in about 12 hours, including calibration and a repeated section for quality control. Data quality was very good, with data profiles repeating to 0.5 percent or better.

4.1.2 GeoBILT Data Collection

We logged two intervals using the GeoBILT system: the complete reservoir (1200-2100 ft) and the main water flooded interval (1400-1800 ft). Data were collected at all four frequencies using the complete (slow) mode and all logs were measured at least twice. These repeated logs helped establish repeatability and identify conditions such as thermal drift and capacitive coupling. The complete set of logs required about 16 hours over two days. The tool worked reliably for the entire survey.

Data processing was completed in two stages: calibration adjustment and tool rotation. In the calibration adjustment, we adjusted the data with respect to measurements made in free space. This is used to calculate the primary field and to adjust for phase shifts. The final processing consisted of tool rotation using the three-component magnetometer data to orient the tool axes to geographic north (*x*-coordinate).

Figure 9 shows apparent resistivity logs, with repeats, from the vertical source and the 2m and 5m offset vertical sensors. We also show the logs from the commercial (Halliburton) deep induction resistivity log, measured several months earlier in the same well. The plots show a good correlation with the commercial log, although both GeoBILT logs are somewhat smoother due to the longer source- receiver

offsets. The slight variation between the repeated logs is most likely due to thermal drift, suggesting that our thermal calibrations need further refinement.

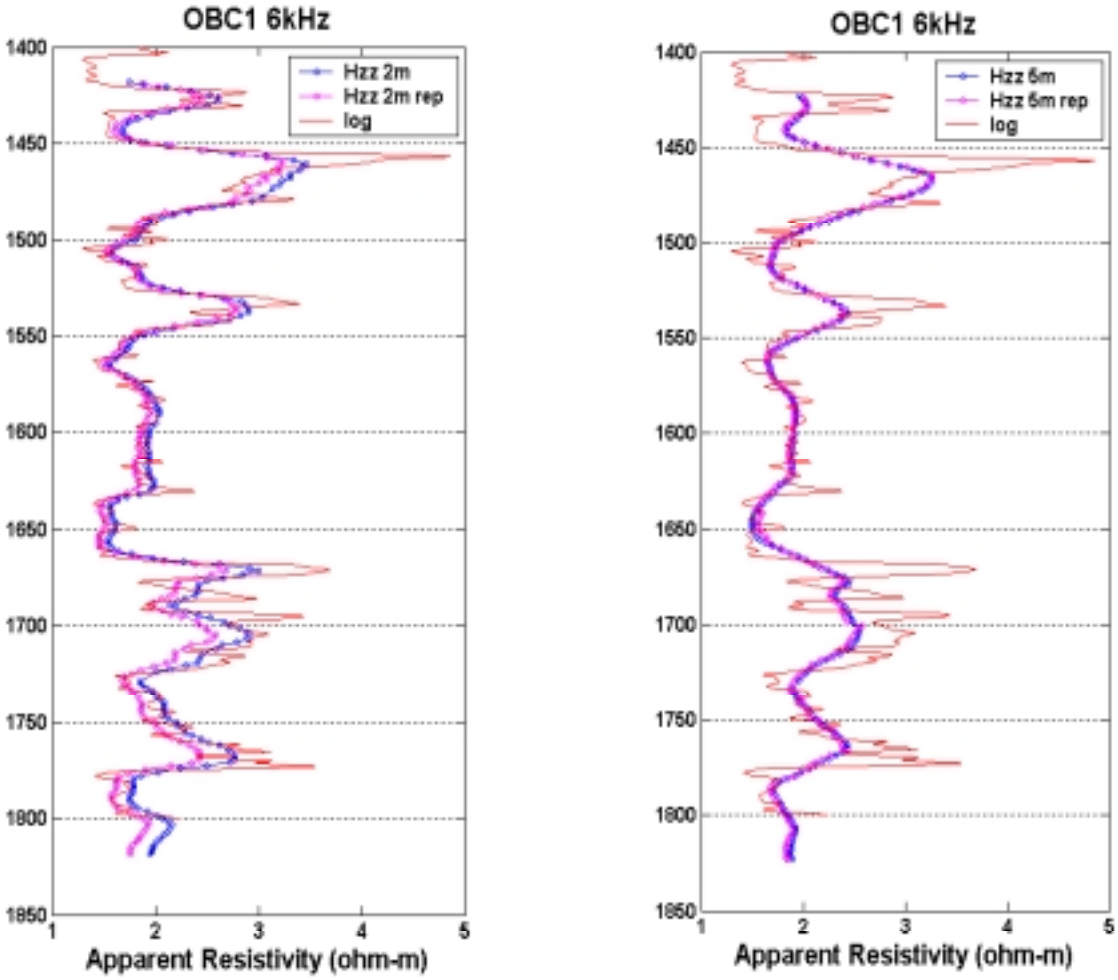

Figure 9. GeoBILT logs of Tz-Rz for 2m and 5m separations, f=6kHz

Figure 10 shows the apparent resistivity logs for the horizontal component, maximum coupled sources and receivers (Hxx and Hyy) in the same well, with repeats. The Hxx and Hyy logs are quite different in appearance to the vertical logs in Figure 9 and somewhat different from each other. The horizontal logs appear sharper and choppier than the vertical logs, and although many layers correlate between the two logs, others do not. Note that the 2m and 5m offset logs appear quite different from each other. The 2m plots are sharper and show larger swings at layer boundaries. We suspect that these logs are responding to the thinner layers.

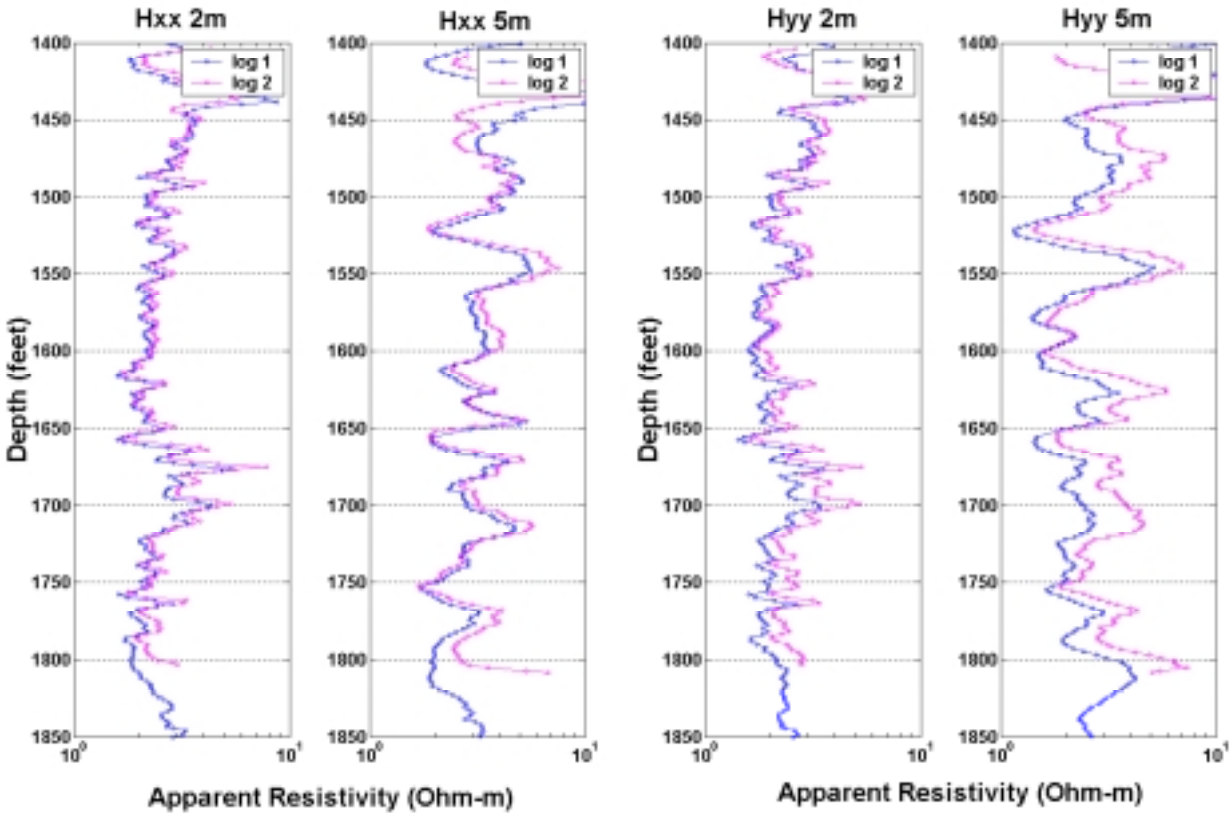

Figure 10. GeoBILT logs from OBC1 Tx-Rx and Ty-Ry for 2m and 5m separations

Notice that the variance of the repeated horizontal logs is considerably higher than the vertical logs. This is probably due to the fact that each log is the rotated resultant of two individual logs. We therefore see the combined effect of the drift on both logs as well as the result of the propagation of any calibration differences between the sensors and sources.

The Hxx and Hyy logs are similar to each other in overall appearance over much of the section but quite different in specific zones. For example, at depths between 1600 and 1750 ft, the logs are quite different in appearance. We note that this depth interval corresponds to the largest water influx from the adjacent water injector, and the differences between the logs might correspond to an injection-induced anisotropy (i.e. 3D structure due to water flooding).

Samples of the null-coupled logs (Hzx and Hzy) are provided in Figure 11. The logs show the amplitude of the horizontal fields from the vertical source for the entire reservoir depth (1200-2100 ft). Note that these fields are theoretically zero for a homogeneous or horizontally layered structure in a vertical well, but they are clearly not zero here. In particular, there are significant anomalies centered at depths 1350, 1450, 1700 and 1925 ft. We note that these depths correspond to layers most affected by water flooding from the adjacent injector (see Figure 7).

We note that the characteristics of the null fields are different in each of these anomalous zones as evident in the variation of the X and Y component logs. This suggests that the flow direction and characteristics are different in each interval. Although the magnitude of these null-coupled fields is quite small, between 0.1 and 2 percent of the direct-coupled field, the repeated logs show that these data are very reproducible. In fact, from these data we estimate that the reproducibility is roughly 500 parts per million.

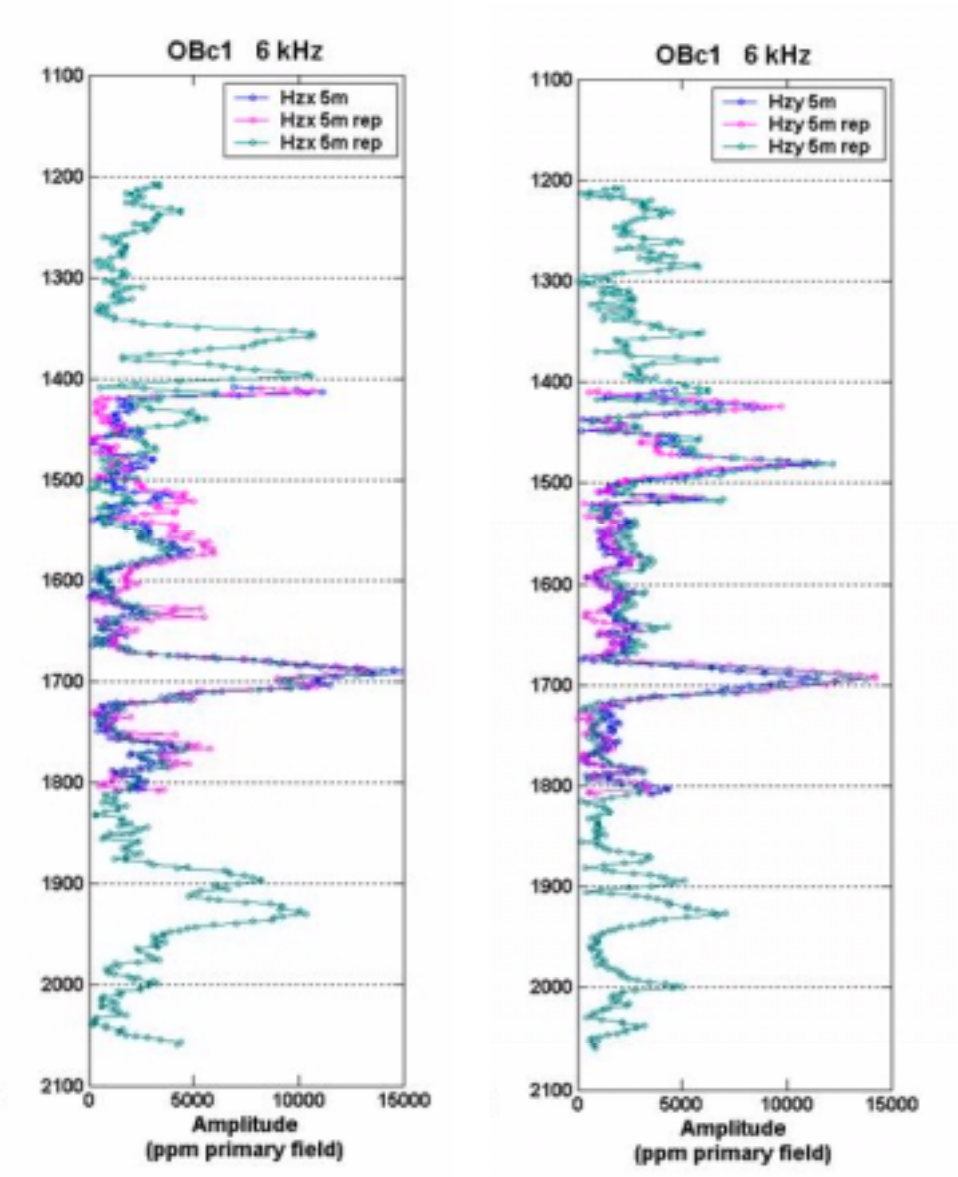

Figure 11. GeoBILT logs of Tz-Rx and Tz-Ry for 5m source-sensor separation

4.1.3 Crosswell and GeoBILT Data Interpretation

Collected crosswell and GeoBILT data were both interpreted utilizing automatic inverse computer codes. For both cases, we assumed a starting model based on the induction resistivity logs. In the crosswell case, we interpolated the logs between the wells for a 2D starting model; for the GeoBILT data, we used the logs to construct a 1D-layered section.

Crosswell data were fit with the 2D inversion code (SINV2D) developed by Sandia lab (Alumbaugh and Newmann, 1996). This code has been used for more than 3 years in crosswell data interpretation (Wilt at al, 2001).

The reservoir stratigraphy at this site consists of a series of 10-80 ft thick units dipping slightly from north to south (OB-C1 to OB-C2). Stratigraphic profiles indicate that the section consists of a relatively constant percentage of shale (illite) and variable amounts of silt and diatomite. Prior to water flooding, the siltier sections tended to have lower resistivities, 1.5-2.5 ohm-m, and the diatomite sections have resistivities that range from 2.5-4.0 ohm-m due a higher initial oil or gas saturation.

Chevron geologists and engineers have divided the reservoir section into approximately 15 correlatable units chosen for differences in composition and log responses. Several of the prominent markers are also shown on the crosswell resistivity section in Figure 12.

In Figure 8, the deep induction logs from wells 11-8W and 11-8WR are shown. These wells are adjacent and situated roughly 40 ft from OBC1. Well 11-8W was drilled in 1994 to supply water for the pilot, and well 11-8WR was drilled in June 2000 to supply CO_2 to the same layers (FF-L). Some of the marker horizons are identified on the plots.

The logs from these adjacent wells can be used to measure changes in resistivity that occurred during the past 6 years of water flooding. We can see that layers H and J have significantly changed. These are 100 ft thick layers of predominantly diatomite. The change is largest in layer H, which shows more than a 50 percent reduction in resistivity over the 6-year period. This corresponds to a 12 percent replacement of void space (or oil) by the injected salt water. In layers F and J, there is a corresponding, but less dramatic reduction. In other layers, for example layer G, it appears that the resistivity has slightly increased during the flooding operations. This may be due to re-saturation.

In Figure 12, we show the resistivity cross section derived from the crosswell EM data between wells OB-C1 and OB-C2. We have placed induction logs 11-8W and 11-8WR within the section for reference. The figures clearly show a roughly flatlying multilayered section throughout much of the image, although there is a clear lateral boundary near well OB-C1 in the deeper parts of the section. Note

that the shallower layers seem to clearly dip north to south whereas in the deeper layers, this dip is much less obvious. It may be that resistivity changes due to the waterflood have obscured the dip in the deeper layers.

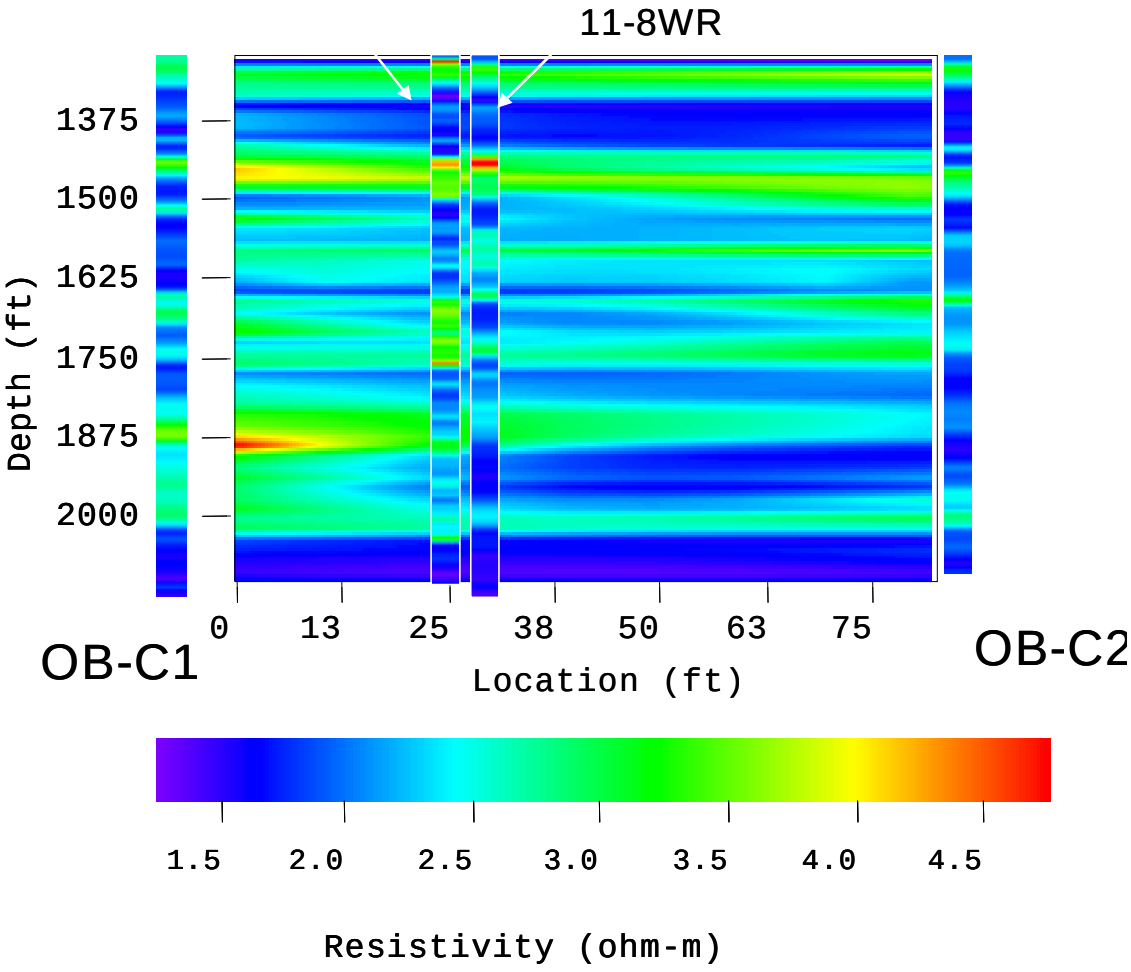

Figure 12. Crosswell EM resistivity section between wells OBC1 and OBC2

Note the difference in resistivity between the borehole induction logs on either side of the image. Well OB-C1 is considerably higher in resistivity than OB-C2, especially at the basal section below 1650 ft. The crosswell section in Figure 7 clearly shows some kind of lateral resistivity change near 15 ft. This probably marks the lateral boundary in the waterflood in layer J. Lateral boundaries are less evident in layers F and H although there are indications of lateral changes at 15ft at depths near 1620 ft and 1700 ft on the section. These boundaries are less clear above and below these depths, indicating that in some sublayers within units F and H, the water moves at a different velocity than in other layers. This is supported by an examination of the logs.

The implication from this image is that the existing waterflood has mainly penetrated into the deeper diatomite rich layers in the section. In these layers, it has reduced the resistivity by up to 50 percent. It also suggests that the edge of the waterflood in these layers is roughly 35-40 ft north of the injector, 15-20 ft south of well OB-C1, and that it has already moved past well OB-C2. Note that the position of this lateral boundary in some sublayers F and H is roughly the same as in J. This suggests that there is some variation among the individual sublayers and evidently poor communication between sublayers.

4.1.4 GeoBILT 3D Data Interpretation

GeoBILT data were fit with a 3D inverse code, INV3D, also developed by Sandia Laboratories (Alumbaugh and Newmann, 1996). Although this code has been used in crosshole and surface data, these are the first single well data used for 3D inversion. Since 3D inversion is very computationally intensive, it is impractical to use it on the entire data set. We therefore focused on the depth interval from 1400-1800 ft, where the largest 3D effects were observed in the data and where there is strong evidence of water flooding at the injection well (Figure 4).

We applied the 3D inversion to the 2 kHz GeoBILT data in the depth interval from 1400-1800 ft as a test. For simplicity, we used only the vertical component transmitter and all three orthogonal receivers at the 5 m offset. These data were fit in stages. We first applied a layered inverse code to fit the vertical component data (ZZ). Using this as a starting model, we fit the null component data to a 3D resistivity distribution. The final solution was then checked against all data. This procedure, although somewhat laborious, was found to be more effective in the long run. Our attempts to fit all data simultaneously produced poor data fits or unreasonable models.

Even for this limited depth interval, the 3D inversion was a lengthy process. Each inverse model required 2-5 days for convergence. In addition, the results were dependent on the weighting of data, the starting model and the noise level and calibration correction of collected data. The results were that numerous runs were made over a two-month period to produce the model shown below.

In Figure 13, we show one planar view and two cross-sectional views of the 3D resistivity distribution near well OBC1 between depths 1400 and 1800 ft. The final 3D model is consistent with the logs and the geology, and the data fit is adequate. The main feature of the model is low resistivity zone that extends southwards and eastward from the well from the well towards the injection fracture.

We note that the logs in Figure 8 show that the undisturbed formation is roughly 4-4.5 ohm-m and the fully swept formation is approximately 1.8 ohm-m. This model shows that well OBC1 is located in a transitional zone between these two extremes.

The injected water is probably not moving as a coherent front; some of the injected saltwater has moved past OBC1 and some has not reached the well.

The map image in Figure 14 indicates that the low resistivity zone is in fact a roughly planar front extending from the fractured injector (upper left hand corner) toward the observation well. We note that the orientation of this front is parallel with the direction of the induced facture, as determined by tiltmeter data.

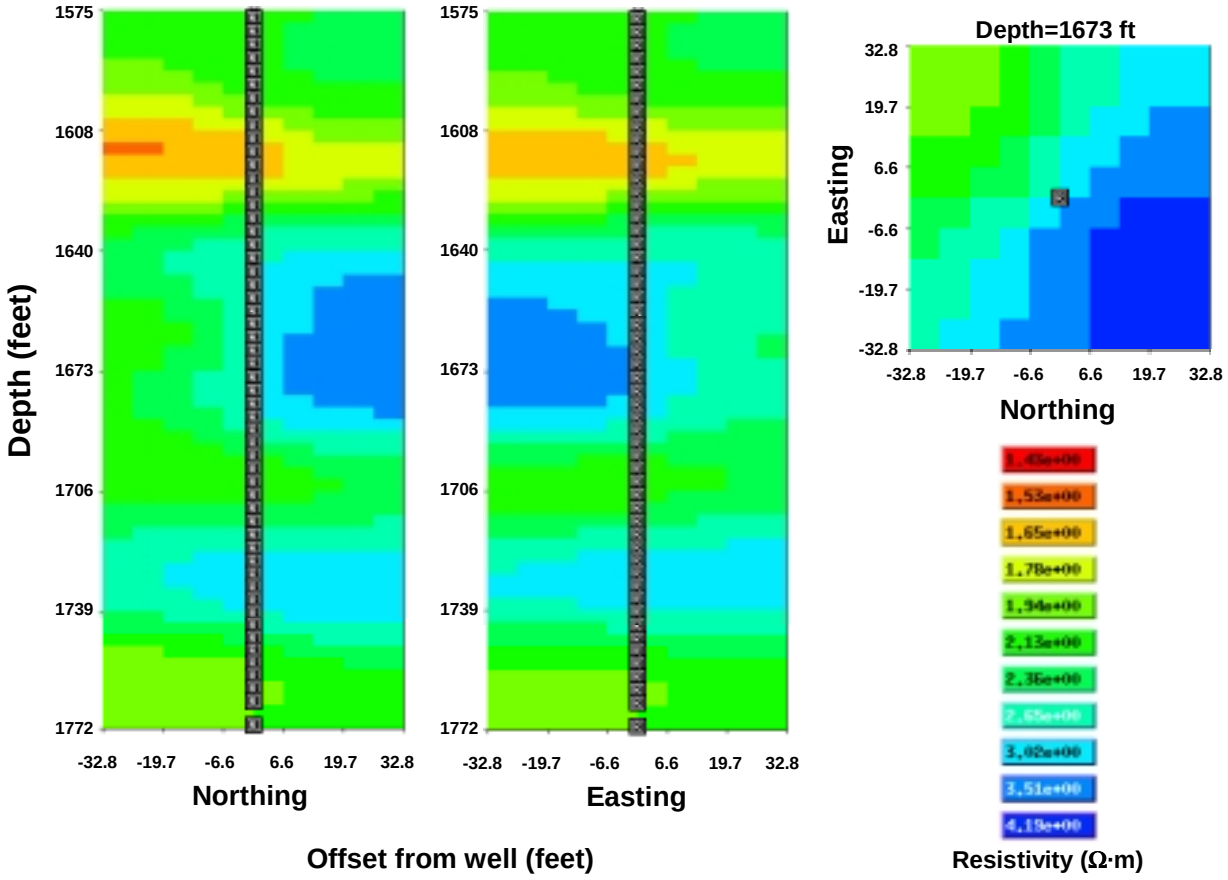

Figure 13. GeoBilt 3D inversion: 2 kHz and 5m transmitter-receiver separations

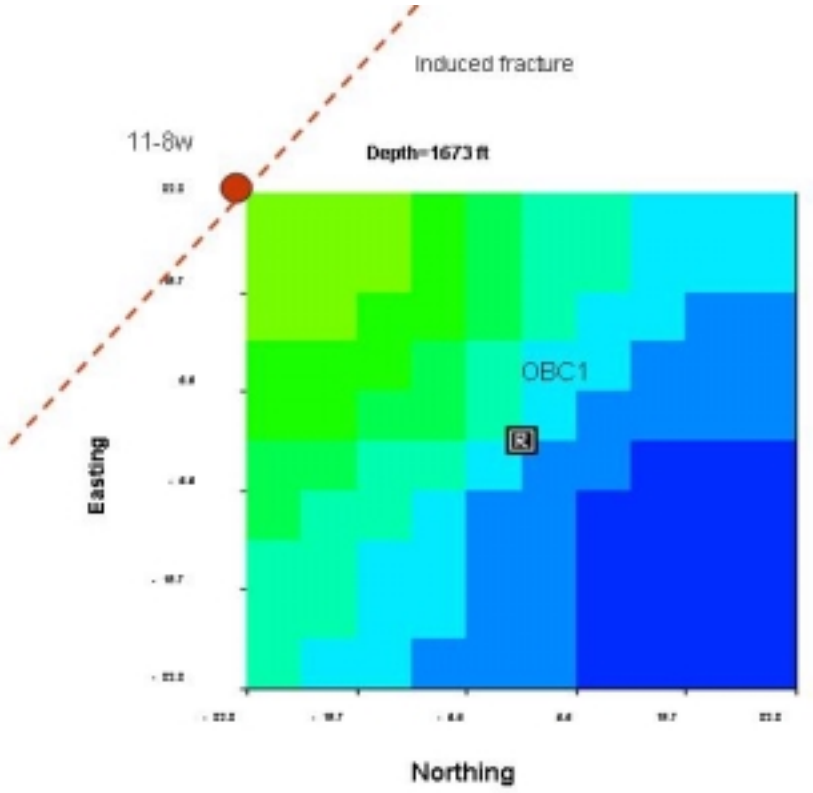

Figure 14. Planar view of the 3D model from GeoBILT data in OBC1

Although computationally expensive, this final 3D image is a consistent with the known geology and provides additional independent data that the water flow is following the induced fracture. This a very satisfying result of 3D image from a single well.

4.2 Case 2: Field Experiment at Dixie Valley, Nevada

Our second field application was in geothermal wells in the Dixie Valley field of central Nevada (Figure 15). In this case, our objective was to operate GeoBILT in a high temperature environment and in an area where the tool could locate near well fractures associated with steam development.

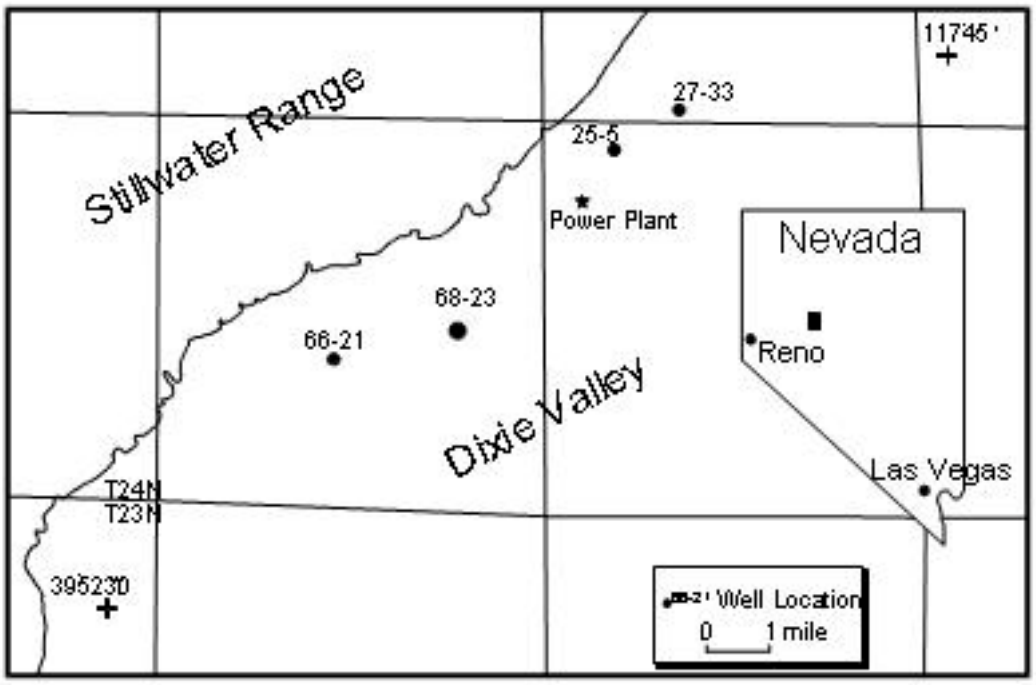

Figure 15. Base map for the Dixie Valley survey

The Dixie Valley geothermal field was discovered in 1970 and has been in operation for more than 15 years. The field is presently operated by Caithness Power LLC and it produces approximately 65 megawatts from a power plant fed by more than 20 wells centered around the present power facility.

Effective steam wells are 8,000-10,000 ft deep and are completed in fractures associated with the range front fault in this basin and range valley. Wells are completed in volcanic and metasedimentary rocks and bottom hole temperatures are from 230-260 ^{o}C. The flow rates are strongly dependent on the nature of the fractures encountered. If the fractures are open, the well can flow at rates exceeding 300,000 lbs/per hour, corresponding to power production of 5-8 megawatts. In some areas, however, the fractures are closed and the wells do not flow.

Wells 66-21 and 68-23 are located 4-6 miles south of the existing producing field along the range front (Figure 15). Both of these wells are hot but neither produces fluids. The bottom hole temperatures in well 66-21 are more than 220 ^{o} C and more than 250 ^{o} C in well 68-23. South of the producing field, where these well are located, there is strong geological evidence for additional steam deposits and several surface manifestations. With one exception, however, the exploration wells in this part of the field are hot but dry.

The stratigraphic section in well 66-21 consists of 4,500-5,000 ft of alluvial sediments underlain by a sequence of volcanic, metamorphic and plutonic rocks. The structural relationships between the various basement rock units is quite complex as evidence by geological studies in the adjacent Stillwater range (ref). The open hole section of the well spans from 7,200-10,000 ft, but there is a constriction at a depth of 8200 ft which makes it impossible to log below this depth. We are therefore restricted to logging to the 1000 ft interval between 7200 and 8200 ft. This interval may be important, however, as there are several zones within these depths where fluid is entering the well.

In Figure 16, we show the original induction resistivity log and a lithologic log in the interval that GeoBILT was logging. The lithologic sequence in this interval mainly consists of metasediments and volcanic rocks with several sequence of granitic rocks, which may in fact be intrusive dikes. The induction log in this interval is fairly nondescript and averages between 50 and 100 ohm-m with the exception of the interval near 7850 ft and the another zone at 7600 ft. Both of these intervals correspond to a change in lithology, from metasediments to granitic rocks. We surmise that there is significant dike intrusion in this interval.

We note that this resistivity log was selected among three provided by Caithness. The logs were surprisingly different from each other, but this particular log seemed to be a more reasonable match to the lithologic section than the other logs. We suspect that the variation between these was due to the hostile downhole conditions which likely influenced the performance of the induction coils used in the logging.

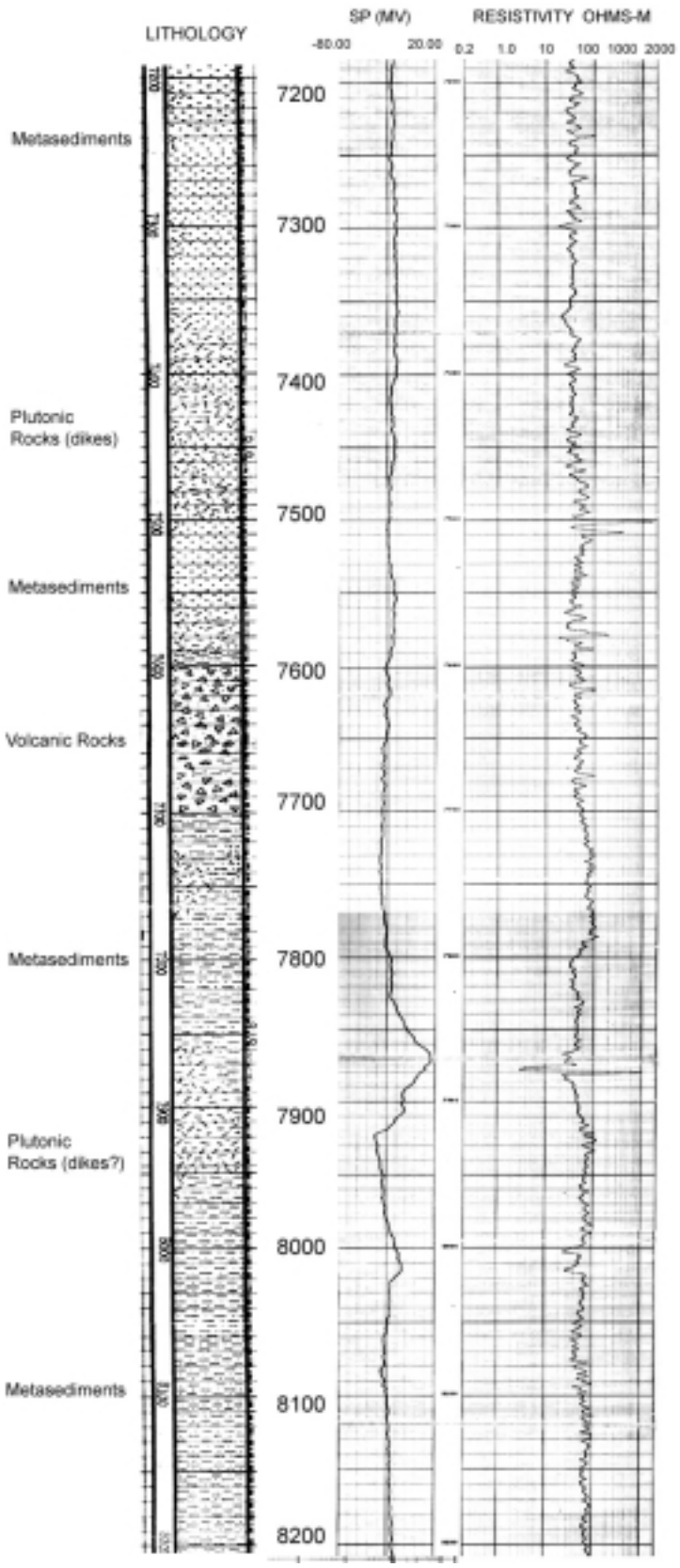

Figure 16. Resistivity and lithologic log

4.2.1 Field Survey

GeoBILT was deployed in well 66-21 on April 10-12, 2002 (see Figure 15). The plan called for the collection of three logs using all field components. Two of the logs would be duplicates so that we can measure the tool repeatability in the high temperature environment. The remaining log was collected at a different frequency.

GeoBILT was deployed using the LLNL logging truck, and a locally rented crane. The well was not pressurized so no lubricators or other pressure protection was required. We operated with a crew of four, two each from LLNL and EMI. The crew was housed in dormitories provided by Caithness Energy at the Dixie Valley power plant. Caithness also supplied support for field operations, including fuel for vehicles and generators, water and other supplies.

Figure 17. Deployment of GeoBILT in well 66-21 in Dixie Valley

During the logging, we kept a close view on the external and internal temperature at the tool. The external temperature ranged from 200 ^{o}C to 220 ^{o}C with the highest temperatures at the bottom of the interval. The internal tool temperature, of the electronic circuits within the insulated dewar, ranged from 60 ^{o} C at the start of logging to more than 120 ^{o}C at the end.

We found that the temperature within the electronics dewar increases at approximately 10 ^{o}C/ hour, allowing us 6-7 hours of logging time per deployment. The tool experienced failures at internal temperatures above 120^{o}C and some of the

electronic components that were rated to125^{o}C failed at those temperatures. One problem is that the receiver section of GeoBILT is powered by batteries and the tool begins to operate (and heat up) as soon as the battery pack is connected. Because the tool must be positioned below a depth of 8,000 ft using a maximum logging rate of 120 ft/minute, this means that GeoBILT is typically powered on for about 2 hours before logging begins. This reducing the logging time to about 5 hours.

The collection of the three logs required about three days, including frequent repairs of electronic components due to temperature induced failures. We believe that the highest quality logs were acquired early in the data collection.

After operations were complete in well 66-21 the tool was deployed in well 68-23. located about 4 miles south of the main field in the dry lakebed at the west side of the valley (Figure 15). This well is deeper and hotter than 66-21 with reported temperatures exceeding 250^{o}C.

We first deployed a dummy tool in well 68-23, to determine the integrity of the well and found that it was open to more than 10,000 ft, although very hot!! We next deployed GeoBILT in the well but the tool failed early in the initial deployment and we were not able to repair it in the field. The survey was therefore terminated at that point.

4.2.2 Data Collection and Interpretation

We present the GeoBILT logging results as a series of apparent resistivity plots for the different field components. The GeoBILT axial logs are equivalent to the standard induction logs, whereas the transaxial and null coupled logs potentially offer new information on the near borehole structure.

In Figure 18, we show the 2m and 5m offset GeoBILT axial apparent resistivity logs collected at 6 kHz in well 66-21.We observe that the axial GeoBILT logs are quite similar to the original induction logs in Figure 16. In this depth interval, the axial logs are largely featureless except for the anomalous zone encountered at a depth of 7860 ft and a smaller one at 8200 ft. It is interesting to note that many of the lithologic units do not have an expression in the axial resistivity logs.

According to the lithology log, the anomalous zone at 7860 ft corresponds to a change from metasediments to a granite diorite. We believe that this boundary probably corresponds to a dike intrusion rather than a stratigraphic boundary.

The transaxial logs show considerably more character and more variation than the vertical logs (Figure 19). We see significant structures at depths of 7450, 7550, 7850 and 8220 ft. The log provides plots for both 6 kHz and 17 kHz measurements and it is clear that they seem to track the same structures.

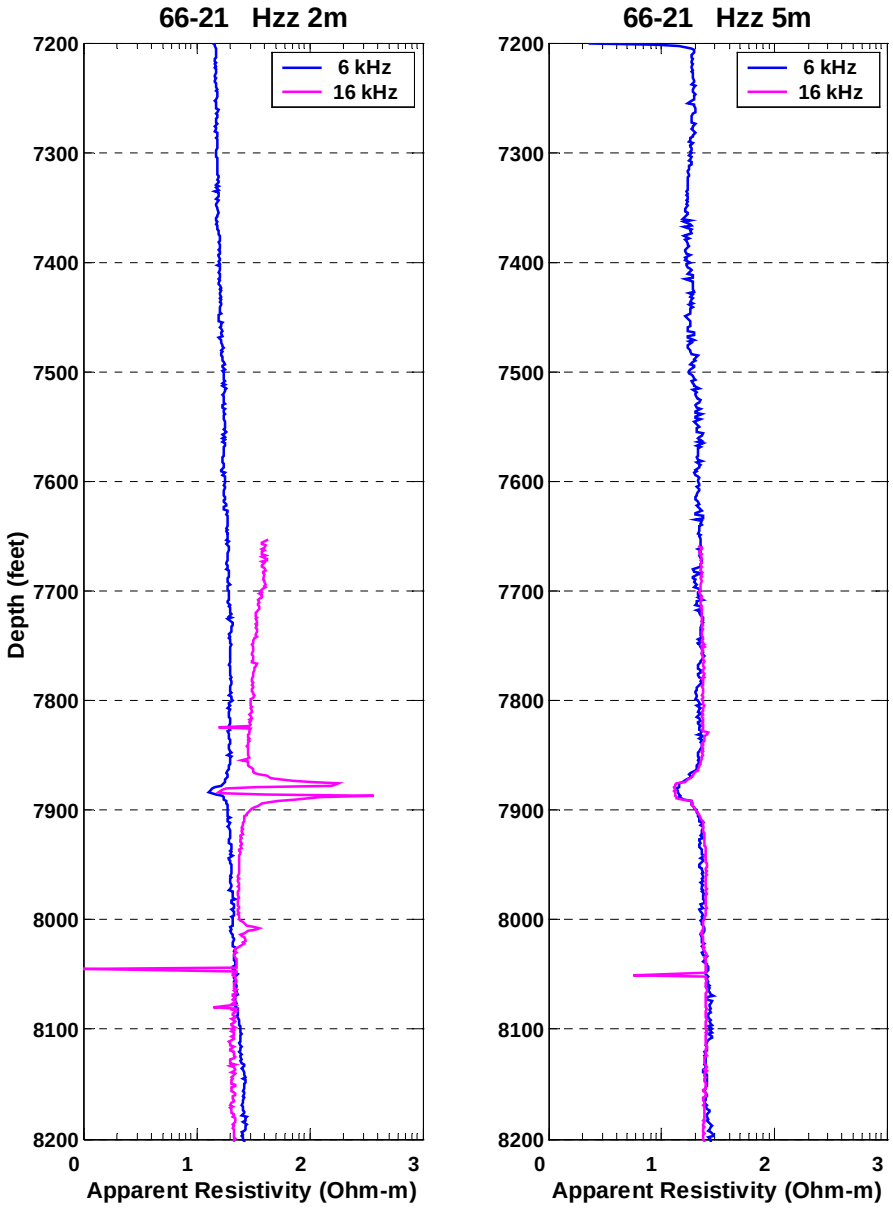

Figure 18. GeoBILT axial apparent resistivity logs, 2m and 5m offset

The clear question is why do the transaxial logs appear to be sensitive to structure transparent to the axial logs. The most likely possibility is that the near well structures are dipping. We note that for a horizontal layer the axial sensors are optimally positioned to induce current into the layer; for a dipping layer this can substantially be reduced and for a vertically dipping layer the transaxial sensors are ideally oriented.

We can test this assertion with a simple model. In Figure 20, we plot the axial and transaxial apparent resistivity logs for a flatlying low resistivity layer in a uniform medium, and for the same model with a 60-degree dip. This layer might represent a thin hot fracture zone, for example. The model uses a 5m source sensor spacing and a frequency of 6 kHz, the same as GeoBILT.

For the flatlying target (model 1), we observe that the axial and transaxial fields produce roughly the same response from the layer. For the dipping target (model 2), however, the transaxial configuration is more than two times as sensitive to the target. This means that for a dipping section the transaxial configuration is more sensitive and more definitive.

The logs and this simple example suggest that the structure near well 66-21 is dipping, at about 60 degrees. The correspondence of the low resistivity zones in the GeoBILT logs with the granitic rock annotated in the lithology log suggests that these granitic zones are probably intrusive dikes. We can get a bit more information by examining the null-coupled logs.

In Figure 21, we show the null-coupled logs ZY logs (Y sensor directed northwards) in this well. The logs represent the signal measured in an orthogonal sensor to the source. The logs are therefore zero in a uniform or layered space but they are very sensitive to nonuniform structure around the wells, such as fractures or steep dip. Typically these logs must exceed 0.5 percent of the direct coupled field to represent significant structure and it is important that the logs be repeated to determine level at which features reproduce. We are gratified that the 6 and 16 kHz null-coupled data agree at levels above 0.5 percent, especially in the ZY component.

We note that the ZY (north receiver) and ZX logs (east receiver) are fundamentally different logs in this well. The ZX log is relatively small for the entire interval, whereas ZY is significant in several intervals. This indicates that the causative structure lies mainly west of the well and there is little component directly to the north.

Examining the lithology logs in Figure 16, we can see a good but rough correlation of the null coupled anomalies and the granitic lithology. This is further evidence that the granitic annotation refers to intrusive dikes and that these dikes are dipping bodies associated with fractured country rock.

We feel that GeoBILT data from these logs in 66-21 provided some new information unavailable from the standard induction logging. GeoBILT provided information on the nature of the anomalies as well as the dip and orientation of the causative structure.

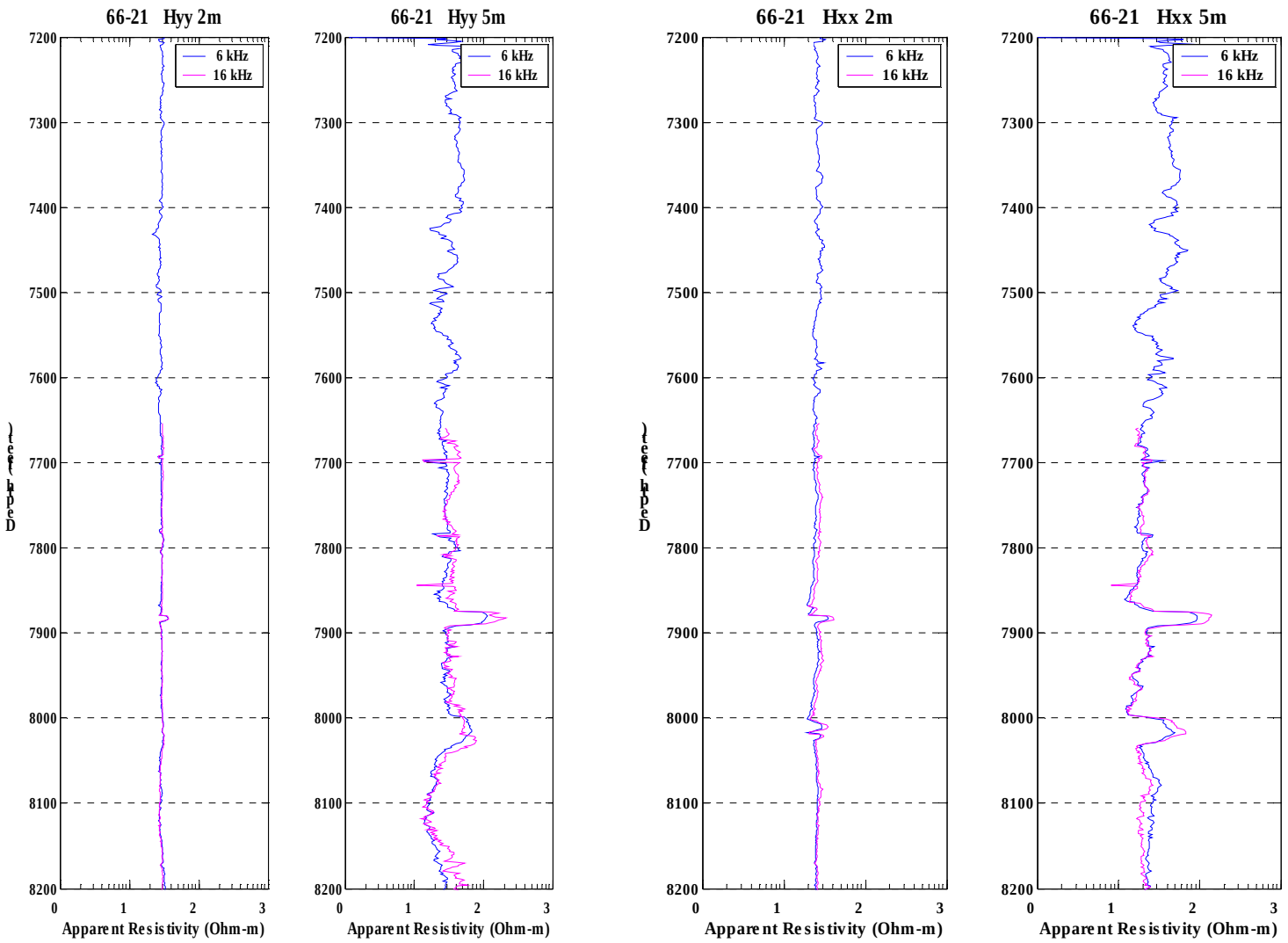

Figure 19. Transaxial logs

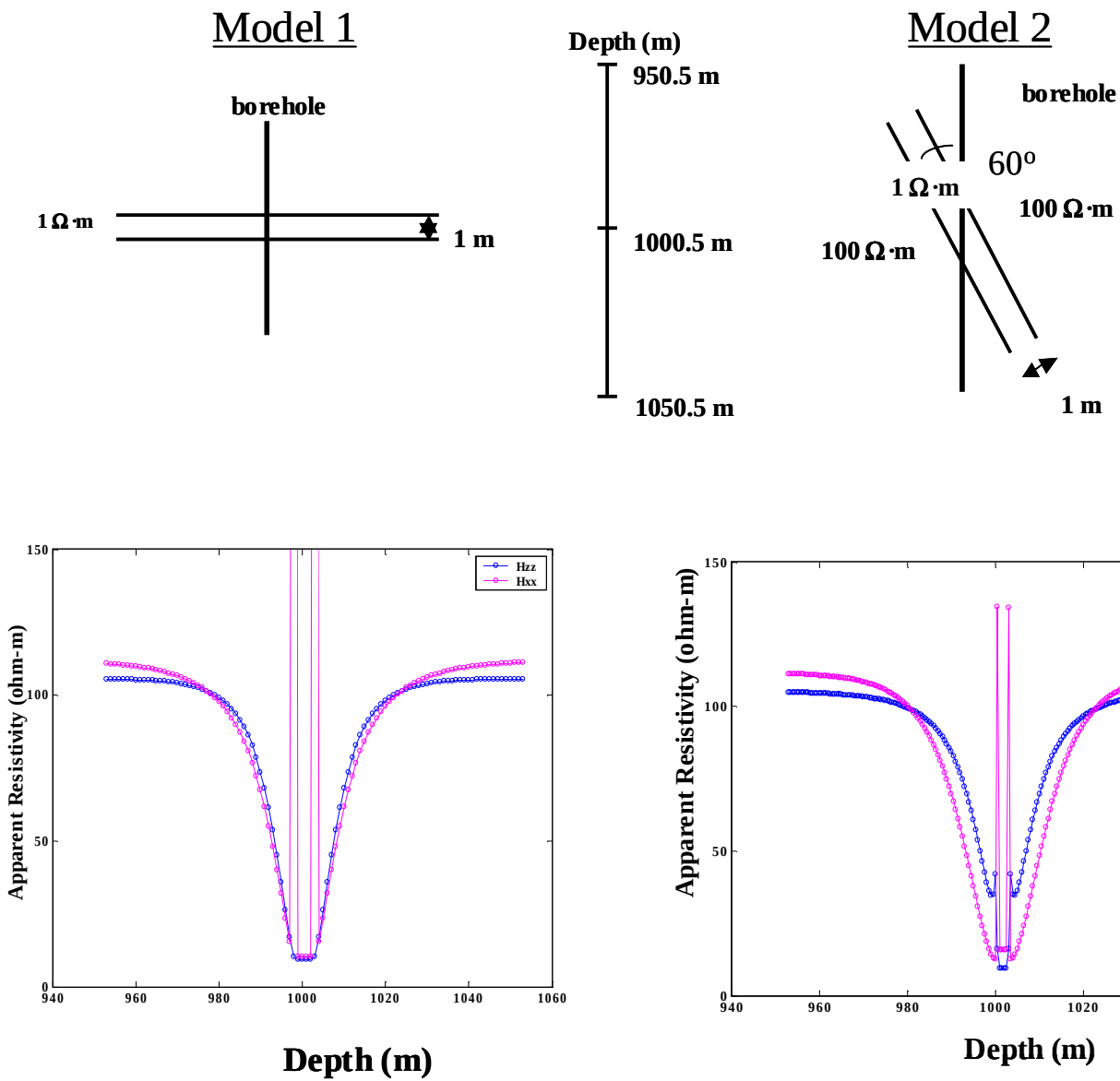

Figure 20. Axial and transaxial apparent resistivity logs for 2 models

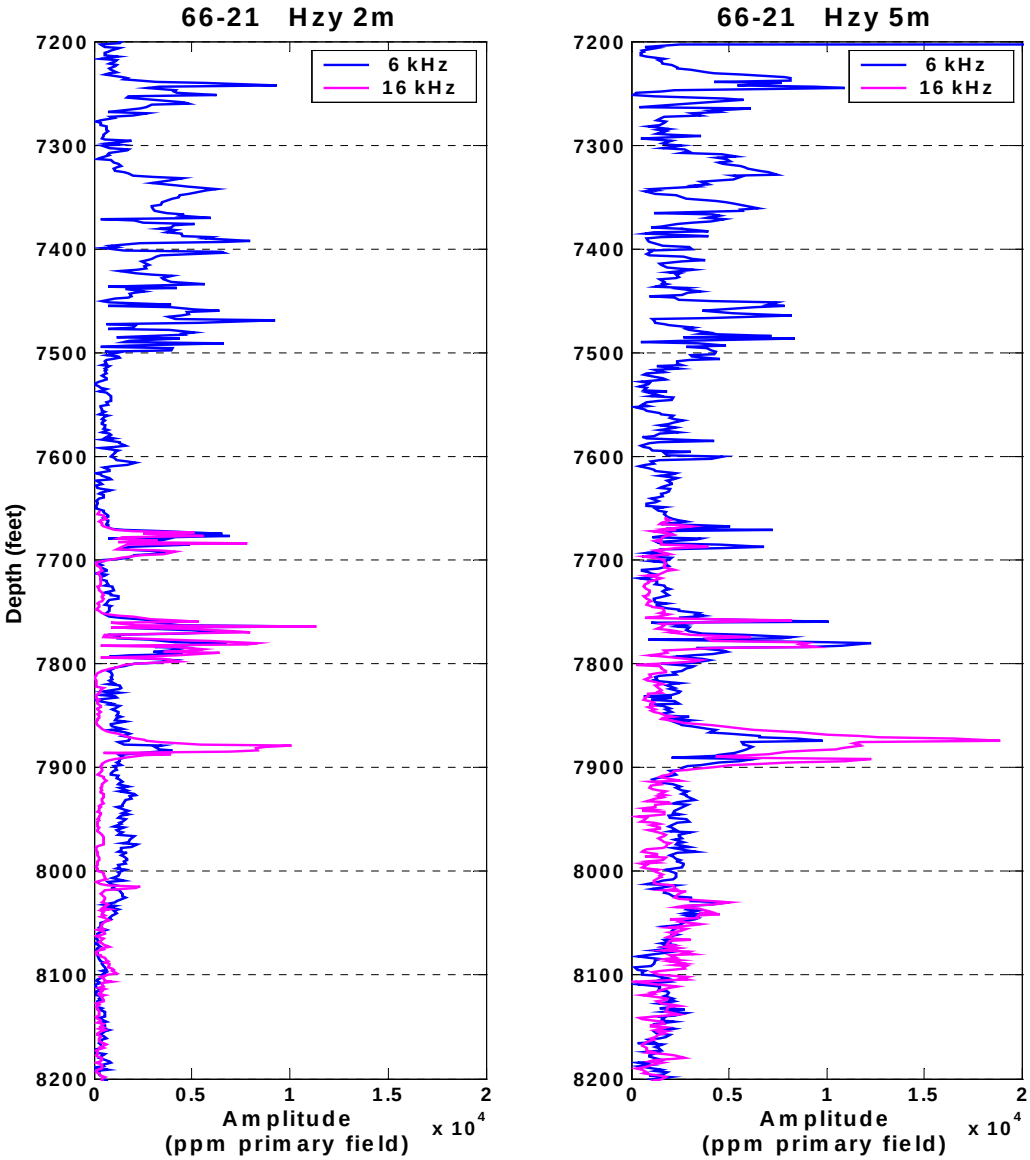

Figure 21. Null-coupled logs

5 Conclusions and Recommendations

The development of GeoBILT was a long complex process that culminated with the manufacture of a working prototype logging device. This device was used in three field trials and in each it provided information unavailable with any other logging technology.

In Lost Hills, we used GeoBILT data to construct a near well 3D resistivity model consistent with water flow from a nearby water injection well. The model is very useful in identifying horizons and flow paths to the water injection used for oil recovery and pressure maintenance.

In the high temperature Dixie Valley geothermal field, GeoBILT data was able identify steeply dipping structure associated with dike intrusion and water inflow in particular depth horizons.

The potential benefits of this technology for both oil and gas and geothermal development are clear. The logs truly make the most of the access provided by the drill hole. GeoBILT can see 2 and 3D formation structure at substantial offsets from the well bore and clearly identify near well fractures.

California is blessed with both petroleum and geothermal resources. It is therefore an ideal environment for a device such as GeoBILT, which has application in both communities. In oil and gas fields, GeoBILT can provide significant benefit in field characterization and in tracking injected fluids such as water, steam or CO_2. Its high-temperature capability makes it particularly useful in tracking steam floods.

In geothermal field, the application is in locating near well producing fractures and in helping determine reservoir structure.. We have demonstrated the sensitivity to such structures in the Dixie valley trials.

Several steps are required for commercialization of this technology. We briefly describe them below but they are provided in more detail in the attached business plan.

- **Continued hardware and software development**

  This technology requires continuous technical development over the next several years. The technology appears quite promising but to make it practical it needs hardware improvements, substantial improvement in interpretation software and better logging capability.

- **Geo-BILT2**

  Among the earliest tasks needed prior to commercialization is to build several more tools to be used in continued field trials. These tools should incorporate improvements envisioned during the testing and field trial of the original tool. These include technology to compensate for sensor drift, improvements in tool deployability, including the possibility of tool makeup at the wellhead, and improvement in tool stability.

- **Additional field trials**

  Field trials are probably the most crucial element of marketing new geophysical technology. The are also the best way to assess the performance of the tool. To assure continuous use of the tool during the trial period the strategy is to identify a potential user and form an alliance for a number of field trials in advance.

- **Commercial partner**

  As described in the attached business plan GeoBILT requires a committed commercial partner for the successful development of as commercial product. We have such a partner in our new parent company Schlumberger.

References

Alumbaugh, D.L. and G.A. Newman, 3D Massively Parallel Electromagnetic Inversion Part B: Analysis of a Cross Well EM Experiment, *Radio Science*, 1996.

Hohmann, G., Electromagnetic Methods in Applied Geophysics, Vol. 1 Theory, Investigations in Geophysics no. 3, *Society of Exploration Geophysicists*, 1988.

Lee , 1988, Computer code EM1D

Lutz, S.J., Moore, J.N. and Benoit, D., 1997, Geologic framework of Jurassic reservoir rocks in the Dixie Valley geothermal field, Nevada: Implications from hydrothermal alteration and stratigraphy: Proceedings of the 22nd Workshop on Geothermal Reservoir Engineering, Stanford University Report SGP-TR-155, p. 131-139

Sato, T., Osato, K., Takasugi, S., and T. Uchida, Development of the Multi-Frequency Array Induction Logging (MAIL) Tool, *Geothermal Resources Council Transactions*, V 20, 637-642, 1996.

Stosur J.J. and A. David, Petrophysical Evaluation of the Diatomite Formation of the Lost Hills Field, California, *Journal of Petroleum Technology*, no.1138, 1976.

Uchida, T., K. Akaku, M. Sasaki, H. Kamenosono, N. Doi, and S. Miyazaki, Recent Progress of NEDO's Deep-Seated Geothermal Resources Survey Project, *Geothermal Resources Council Transactions*, v 20, p. 9, 643-648.

Wilt, M, P. Zhang, M. Morea, D. Julander, and P. Mock, Using Crosswell Electromagnetics to Map Water Saturation and Formation Structure at Lost Hills, *SPE Regional Meeting Bakersfield, Ca*, paper number 68802, 2001.

Papers published and presentations given as part of this project:

Alumbaugh D.L. and M. J. Wilt, A Numerical Sensitivity Study of Three Dimensional Imaging from a Single Borehole, *Petrophysics*, 42 no.1, pp19-31, 2000.

Wilt, M., R. Mallan, P. Kasameyer, and B. Kirkendahl, 3D Extended Logging for Geothermal Resources: Field Trials with the GeoBILT System. *Stanford Geothermal Workshop*, January 2002.

Lee, Ki Ha, Kim, Hee Joon, and Michael Wilt, 2002 Efficient imaging of single-hole electromagnetic data . Su8bmitted to 2002 Geothermal Resources Council Annual Meeting.

Mallan, R., Wilt, M., Kirkendahl, B., and Osato, K., 2000, Subsurface Electrical Measurements in Dixie Valley using Single Well and Surface to well Induction logging, Proceedings, Twenty-Sixth Workshop on Geothermal Reservoir Engineering Stanford University, Stanford, California,.

Wilt., M Takasugi. S., Uchida, T., Kasameyer, P. Lee K. and Lippmann, M., 1997, Fracture Mapping In Geothermal Fields with Long-Offset Induction Logging, Proceedings from 22 nd Stanford Geothermal Conference on Geothermal Reservoir Engineering, paper number SGP-TR-155.

Appendix A. Technical Description of GeoBILT

The hardware part of the system is mainly composed of the surface station, the surface computer and the downhole tool. The station has a depth counter and power supply while the computer controls the whole system and runs software programs for system operation, data control, data processing and interpretation.

The downhole tool has dimensions and connections that fit the industry standard 7-pin Gerhardt-Owens cable connector. All parts are hardened against high temperature, high pressure and corrosive environment. It operates in boreholes with temperatures of up to 260 ^{o}C and oil production depths of up to 4 km.

The two main parts of the tool are: the Transmitter (Tx) Sonde and the Receiver (Rx) Sonde. Each sonde has its own sensor (or source) amplifier and/or driver electronics, and a digital acquisition module with an in-tool computer to control data collection. All in-tool computers are connected via a downhole local area network (LAN) for higher communication speed between modules.

GeoBILT's unique feature, the 3-component transmitter combined with the 3-component receiver, provides for the collection of nine-component *vector* data sets. These data are crucial for the delineation of off-axis structures such as fractures and reservoir inhomogeneities.

The downhole tool is a modular system designed for easy maintenance and future upgrades. The tool module spacing, operating frequencies, and type of sensor and source can be configured in a variety of ways to fit individual environments.

A diagram of the main parts of GeoBILT is shown in Figure A22.

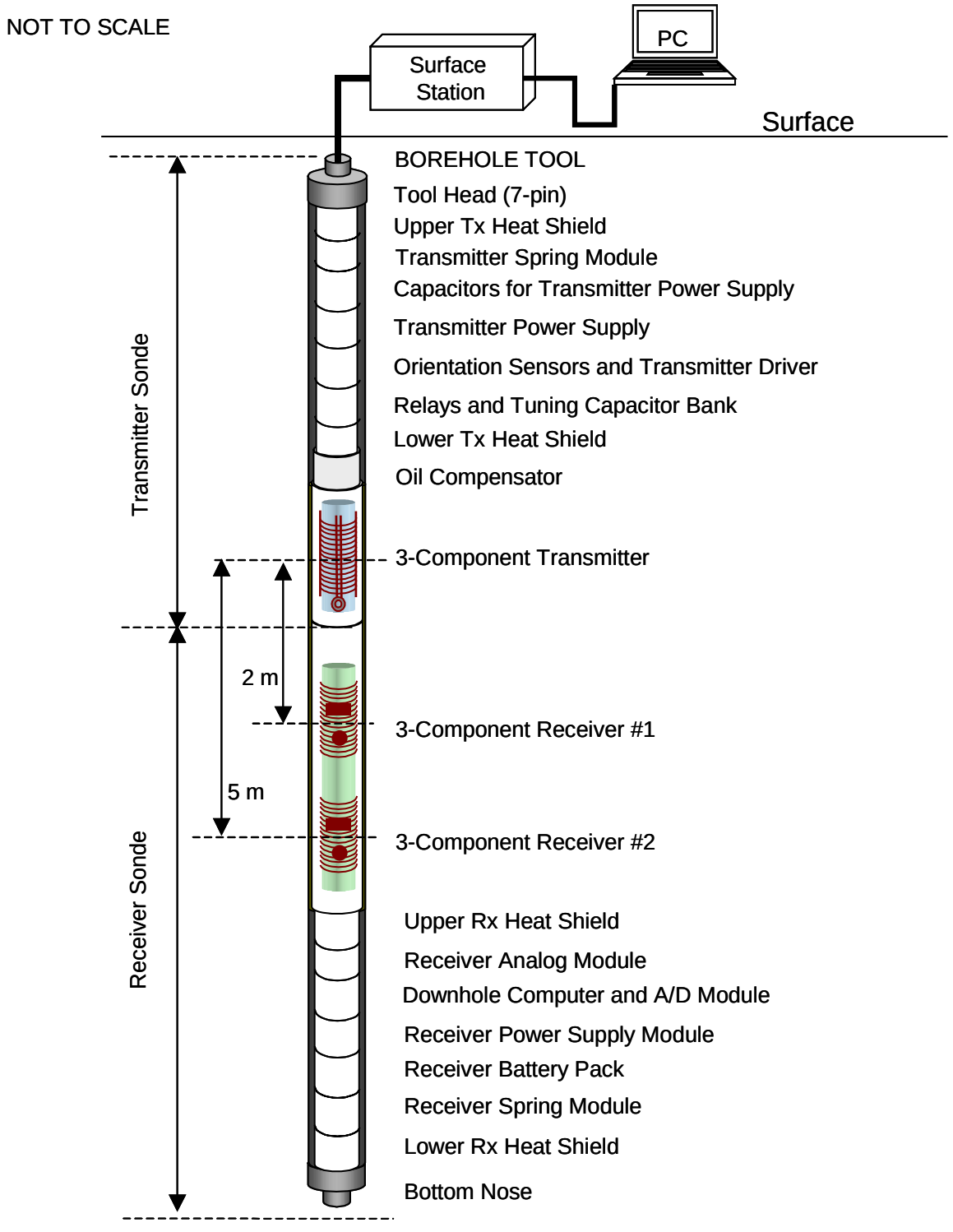

Figure A22. Diagram of GeoBILT system, showing main parts

A.1 Surface Equipment

A.1.1 Surface Station

The surface station has an external Sorensen 600V/1.7A DC Power Supply for the downhole transmitter. In addition, it has a digital depth counter for reading the depth of the tool, an electronics board for communicating with the tool, a second electronics board for controlling the Sorensen DC Power Supply output, an internal triple output DC power supply for the electronics boards, and a +5V output for the winch optical encoder. To connect with the surface computer, there are two communication ports in the back panel of surface station. It also provides status lights and tool status diagnostics.

A.1.2 Surface Computer

Any commercially available portable computer may be used for this purpose. The surface computer controls the system and collects data from the downhole tool. Specifications required are:

- 2 serial communication ports via a PCMCIA card
- Processor speed of at least 100 MHz
- Minimum 32 Mbytes of memory and 2 GB hard disk

In addition to data collection, some data processing is also done on the computer. This includes data editing, calibration correction, and re-sampling for subsequent inversion.

Figure A23. GeoBILT surface station and surface computer

A.2 Transmitter Sonde

The Transmitter Sonde consists of four main sections: the tool head, Tx electronics section, oil compensation unit, and the Tx antenna assembly.

A.2.1 Tool Head and Heat Shield

The tool head is a mechanical assembly without any electrical components. It connects the tool body to the logging cable via a standard Gerhardt 7-pin connector.

The upper Tx heat shield is a detachable fiberglass piece that is immediately attached to the tool head.

A.2.2 Transmitter Electronics Section

The Tx electronics section contains five modules, each packaged within a separate canister. The base chassis inside the canister is a single machined and welded part, and terminates with male/female connectors. The electronics are secured to the chassis with a steel housing. See Figure A24 below.

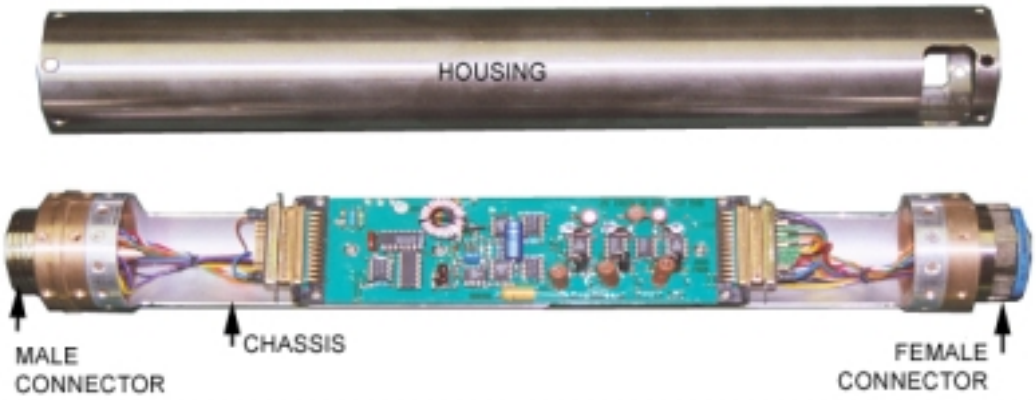

Figure A24. Electronics packaging

The assembled modules are further housed in a stainless steel thermal dewar that connects with the tool head. The make-up length of the upper end (tool head and Tx electronics section) is about 12 ft.

Following are descriptions of each transmitter electronic module.

Transmitter Spring Module
This is a spring-loaded mechanical device that adds strength and rigidity to the assembled electronic modules. The upper Tx heat shield plugs into this module and the connector is locked mechanically.

Capacitors for Transmitter Power Supply
This module encloses the capacitors used for the Tx power supply.

Transmitter Power Supply
The Tx power supply regulates and distributes the input voltage supplied by the surface-based DC power. This module provides regulated power to all transmitter electronics.

Orientation Sensors and Transmitter Driver
This module is the operational center of the Transmitter Sonde. It includes tool orientation magnetometers, accelerometers, voltage and current monitors, and various temperature sensors that collect data from the array of sensors.

This module has a communication board to hook up the surface station and the receiver downhole computer. There is a transmitter driver circuit which develops a current signal to drive the antenna at frequencies specified by the Rx CPU module.

By alternating between positive and negative power supply voltages, the driver circuit operates as a power supply switch used to develop square wave signals at specified frequencies. The circuit is an extremely efficient signal generator, losing less than one percent of generated power to heat. The transmitter coils are tuned with capacitors and the broadcast signals are sinusoidal as a result of the resonantly tuned circuit.

Relays and Tuning Capacitor Bank
There is an array of capacitors and relays immediately below the driver. These components are used to resonantly tune the transmitter coil for maximum output at the specified frequency. Because of the large inductance of the transmitter coil, its output is severely limited at higher frequencies. In fact, it is a natural LR low pass filter.

Including capacitance in the circuit can compensate for this effect. Using Equation 1 below, a capacitor will resonantly tune the circuit at one frequency for effective cancellation of the impedance due to the source coil inductance.

Equation 1. Tuning Frequency

$$F_C = 1 \Big/ \sqrt{LC}$$

The tuning frequency is given where L is the coil inductance and C is the capacitance of the capacitor array. As we switch between capacitors, the circuit is tuned at different frequencies.

The GeoBILT system has 4 frequencies. Capacitors and coil windings are switched in and out of the circuit using a series of relays controlled by commands from the Rx CPU Module and the Relays Module.

Lower Transmitter Heat Shield
This is a thick fiberglass piece with metal holders. Once connected with the Relays Module, the lower Tx Heat Shield is secured by screws.

Oil Compensation Unit
The Oil Compensation Unit is mounted at the top end of the Tx Antenna Assembly. It equalizes the inner and outer pressures of the tool by keeping the oil in the antenna sections at the same pressure of the outside environment.

The Oil Compensation Unit consists of a toroid-shaped piston mounted on an inner cylinder for feed thru wires. One side of the piston is in contact with the borehole fluids through a set of mesh filters; the other side is in contact with the oil that fills all the free space in the transmitter and receiver antennas.

A.2.3 Transmitter Antenna Assembly

The transmitter consists of three coils, one vertical (*z*T) and two horizontal (*x*T, *y*T), wound in a 3D orthogonal configuration on a fiberglass base. Below these windings are three additional small coils with toroid cores. These are the Flux Monitors, used for monitoring the transmitter's magnetic output or flux.

The antenna assembly is housed in a polyamide housing and filled with oil for pressure compensation and heat dissipation.

A.3 Receiver Sonde

The Receiver Sonde consists of two Rx antenna assemblies, the Rx electronics section and the bottom nose. The receiver antennas are attached to the transmitter and share the same oil compensation unit.

A.3.1 Receiver Antenna Assembly

GeoBILT has two 3-component receiver assemblies located 2 m and 5 m away from the center of the transmitter (see Figure A22). Each antenna assembly contains one axial receiver coil with air core and two transverse coils with mu-metal core. This combination allows for a complete measurement of the magnetic field vector.

The outer diameter of the tool restricts the length of the transverse coils to 2.275 inches. Housing for the antenna is made of polyamide. To compensate for the external pressure, the receivers use the same oil compensation system attached to the transmitter.

The upper Rx heat shield is mounted at the lower head of Receiver #2. It is non-detachable once installed.

A.3.2 Receiver Electronics Module

The Rx electronics section contains five modules, each packaged in a separate canister. The canisters are fastened together by screws and housed in a stainless steel thermal dewar that connects with the Bottom Nose. The total length of the lower end (Rx Electronics Section and Bottom Nose) is about 12 ft.

The modules are further described in the following subsections.

Analog Electronics Module

Immediately below the upper Rx heat shield is a series of circuits for conditioning the analog signal detected in the receivers. These analog circuits are a set of computer-controlled amplifiers and filters to boost signal levels and remove noise from the downhole sensors.

The amplifiers are specifically designed to match each coil to obtain the maximum signal-to-noise ratio over the frequency band of interest. The analog module also includes several amplifier gain and multiplexer options accessed through the software program.

Receiver CPU Module

The CPU module is a set of circuits that controls downhole operation and collects data from the array of sensors. These sensors include the three flux monitors, six receiver coils (nine for future attachment of the 3-component Receiver #3), and various voltage monitors and temperature sensors.

The contents of this module are: a downhole computer (386 PC), a field programmable gate array (FPGA) for timing and I/O controls, four channel A/D circuits, and a communication modem. The firmware sets the operating frequency and multiplexes the 12 signals (3 transmitters and 6 receivers) in all possible combinations into the four-channel A/D converters.

The downhole CPU performs the following functions:

- Frequency selection
- Selection of tuning capacitors
- Control of timing
- Setting of averaging parameters
- Stacking and averaging of flux monitors and receiver waveforms; and Fourier transformations to obtain real and quadrature voltages
- Control of downhole modems to send and receive data to/from the surface

Receiver Power Supply Module

In this module, the powers coming from the in-tool batteries are regulated and distributed to various circuits. The module has three regulated outputs: digital +5V for digital circuits inside the CPU Module, analog +5V and analog –5V for the CPU and Analog Modules.

Receiver Battery Pack Module

There are two battery packs inside this canister to provide power for the digital and analog circuits in the Rx Sonde. The digital battery pack contains 15 C size alkaline batteries and the analog pack has 10 C size alkaline batteries, five for +5V and five for –5V.

For each new battery pack, the nominal voltage is 7.5V. The digital pack may last for about 30 hours, while the analog ones should last at least 5 times longer. The life of the digital battery pack is displayed in the battery voltage monitor on the data acquisition software.

Receiver Spring Module

This is a spring-loaded device that provides additional strength to the electronics section.

Lower Receiver Heat Shield and Bottom Nose

The lower Rx Heat Shield is detachable and should be connected to the Bottom Nose before assembly with the receiver dewar. This module is similar to the upper Tx Heat Shield but positioned upside down.

A.4 Software and Firmware

The GeoBILT software for the surface computer is written in C^{++}, FORTRAN, and MATLAB in a Win98/ Win2000 environment. The programs perform the following functions:

- Initiate data collection
- Select profile parameters (frequency, gains, etc.)
- Display and store data
- Monitor and display downhole conditions
- Read and display tool depth and cable rolling rate information

Once data collection is complete, the data reduction software is used. This program edits raw data and removes bad points, applies calibration corrections and resamples corresponding data to input criteria for the inversion codes. The data set is then fitted to a model of the borehole conductivity structure using an inversion code. The program for this is also supplied with the system.

For the firmware, the following routines are written in C for the downhole processors in the Rx Sonde:

- Controls of downhole relays and switches for frequency selection in the Tx Sonde; amplifier gains setting in the Rx Sonde
- Clock settings and multiplexer controls
- Data initiation and waveform stacking
- Fourier transform of waveforms to real and quadrature voltages
- Message passing to/from the Surface Station
- Requesting orientation data from the Tx Sonde

Appendix B: Induction Logging Principles

A simplified borehole induction tool is comprised of an induction coil (multiturn wire loop) at one end that serves as a transmitting antenna and a second induction coil at the other end that serves as a receiving antenna. The transmitting antenna generates an electromagnetic field in the electrically conducting earth around the borehole, thereby inducing secondary (eddy) currents to flow.

At the receiver end, the measured field includes both primary (generated) and secondary (induced) components. If the primary field is subtracted from the data, the remaining field (secondary) is a direct indicator of the subsurface electrical conductivity around the borehole. At close source-receiver separations, it is usually assumed that the electrical conductivity is uniform and approximates that of a continuous wholespace. The measurements are then converted from electromagnetic field to electrical conductivity by utilizing a simple formula for a homogeneous wholespace earth.

Commercial tools are quite a bit more complex than what is described above but they work on the same principle. For example, in some commercial tools a number of additional transmitter or receiver coils are located along the tool to *focus* on narrow sections. Note that by further separating the source and receiver coils, the log can investigate deeper into the formation away from the well. In any case, however, existing well logs do not penetrate into the formation more than a meter or so from the borehole.

All existing commercial tools utilize axial loop sources and receivers. In typical layered formations encountered in petroleum reservoirs, the induced currents flow parallel to the bedding and the response depends only on the formation resistivity in this direction. If the resistivity perpendicular to the bedding is different, as it is in anisotropic shales if the section has many thin beds, or if there is fracture zone at an angle to the drill hole, it is not possible to determine these properties from the standard tool response.

The addition of vertical loop antennas in GeoBILT induce currents to flow in the vertical direction, across bedding planes, and thereby permit the measurement of formation anisotropy. By inducing the currents to flow in three directions and by measuring the three components of magnetic field, it is possible to deduce the orientation of nonhorizontal structures such as fracture zones, dipping layers or anisotropic formations.